CELLULAR BASIS OF BEHAVIORAL CIRCADIAN RHYTHMS IN MAMMALS-
THE ROLE OF NEUROMEDIN S (NMS)-PRODUCING CELLS IN THE
SUPRACHIASMATIC NUCLEUS

APPROVED BY SUPERVISORY COMMITTEE

Masashi Yanagisawa, M.D., Ph.D. (Co-Mentor)

Joseph S. Takahashi, Ph.D. (Co-Mentor)

Joel K. Elmquist, D.V.M., Ph.D.

David Russell, Ph.D.

Robert Greene., M.D., Ph.D.

ACKNOWLEDGEMENTS

I would like to thank my advisors, Dr. Masashi Yanagisawa and Dr. Joseph Takahashi for their assuring guidance, patience, and wisdom. The experiences that I've gained from working in not one but two of the most distinguished laboratories in this world are something that I will never take for granted. I am truly thankful for their mentorships throughout my graduate career and can only aim to one day become half as intelligent and accomplished as they are. I would also like to thank members of my dissertation committee, Dr. Joel Elmquist, Dr. David Russell, and Dr. Robert Greene for providing valuable scientific advice and constructive criticisms these past few years.

I have received an extraordinary amount of support from members of both the Yanagisawa lab and the Takahashi lab. I like to thank current and past members of Yanagisawa lab, including Shelley Dixon, Toshiyuki Motoike, Alexander Chang, Yuichi Ikeda, Hidetoshi Kumagai, Randal Floyd, Makito Sato, Amber Skach, Ayako Suzuki, Marcus Thornton, Kathleen Godwin, Manabu Manandhar, John DuBose, Taizo Matsuki, and Stephanie Baldock. I would like to especially thank Yuichi Ikeda, Hidetoshi Kumagai, Alexander Chang, Toshiyuki Motoike, and Shelley Dixon for their tremendous contribution to my education in science and in life and to this dissertation. Without your constant guidance and encouragement, this dissertation would not have been possible. Our conversations, discussions, and camaraderie in and out of the lab are memories that I will cherish for the rest of life. I would like to also especially thank Manabu Manandhar, whom I had the pleasuring

of supervising. Without his enthusiastic efforts and companionship, the research presented in this dissertation would not have been where it is now. I like to thank him for working hard with me through the good and the bad times. I like to thank current and past members of the Takahashi lab, including Seung-Hee Yoo, Shuzhang Yang, Jennifer Mohawk, Yongli Shan, Guocun Huang, Yan Li, Junmei Fan, Izabela Kornblum, Jeffrey Seinfeld, Vivek Kumar, Neha Kumar, Yogarany Chelliah, Nobuya Koike, Kyung-in Kim, Marleen De Groot, Mariko Izumo, Lisa Thomas, Chryshanthi Joseph, Hee-Kyung Hong, Lucia Pagani, and Michael Wellems. I would like to especially thank Shuzhang Yang, Jennifer Mohawk, Seung-Hee Yoo, and Yongli Shan for their generous and dedicated instructions, advices, encouragements, and technical support. Their eagerness to guide and help me made this dissertation possible. Last but not least, I want to thank God, my mom, my dad, and my wife, Yuka, for their loving support.

CELLULAR BASIS OF BEHAVIORAL CIRCADIAN RHYTHMS IN MAMMALS- THE ROLE OF NEUROMEDIN S (NMS)-PRODUCING CELLS IN THE SUPRACHIASMATIC NUCLEUS

by

IVAN T. LEE

DISSERTATION

Presented to the Faculty of the Graduate School of Biomedical Sciences

The University of Texas Southwestern Medical Center at Dallas

In Partial Fulfillment of the Requirements

For the Degree of

DOCTOR OF PHILOSOPHY

The University of Texas Southwestern Medical Center at Dallas

Dallas, Texas

May, 2013

CELLULAR BASIS OF BEHAVIORAL CIRCADIAN RHYTHMS IN MAMMALS-
THE ROLE OF NEUROMEDIN S (NMS)-PRODUCING CELLS IN THE
SUPRACHIASMATIC NUCLEUS

IVAN T. LEE

The University of Texas Southwestern Medical Center at Dallas, 2013

Supervising Professor: Masashi Yanagisawa, M.D., Ph.D. (Co-Mentor) and
Joseph S. Takahashi, Ph.D. (Co-Mentor)

ABSTRACT

Behavioral circadian rhythms in mammals are controlled by highly heterogeneous populations of neurons located in the suprachiasmatic nucleus (SCN). Lesion and transplantation studies have established that the SCN is both necessary and sufficient for the generation of daily rhythms in locomotion. It remains uncertain, however, whether this pacemaking property of the SCN is limited to certain subsets of cells or intrinsic to all neurons within the SCN. To dissect out the cellular properties of circadian rhythms, we utilized a BAC transgenic mouse line in which Cre recombinase (iCre) is driven by the promoter of *neuromedin S* (*Nms*), a neuropeptide that has restricted expression in ~40% of

cells within the SCN. Using this cell-type specific driver, we genetically altered the molecular oscillation of *Nms*-positive cells by overexpressing the $Clock^{\Delta 19}$ or the *Period2* transgene. $Clock^{\Delta 19}$ is a semi-dominant mutation that leads to lengthened behavioral circadian periods when expressed in the majority of SCN cells. Likewise, *Period2*, when overexpressed in all or almost all of the SCN neurons, lead to the loss of behavioral circadian rhythms. We found that, intriguingly, the transgenic expression of $Clock^{\Delta 19}$ only in *Nms*-positive neurons leads to a lengthened period in circadian rhythms while the overexpression of *Per2* in *Nms*-expressing neurons causes the loss of daily rhythms altogether, suggesting that behavioral rhythms can be controlled by the molecular oscillation of *Nms*-positive cells. Next, to ascertain whether *Nms*-expressing neurons are required for normal behavioral circadian rhythms, we utilized a tetanus toxin-based technology that permits the inducible and reversible inhibition of neurotransmission. Surprisingly, this genetic manipulation revealed that synaptic neurotransmission from *Nms* neurons is essential for the generation of behavioral circadian rhythms. Taken together, these results indicate that *Nms* marks a specialized subgroup of neurons that is both necessary and sufficient for the production of circadian rhythms in behavior.

TABLE OF CONTENTS

LIST OF FIGURES

LIST OF TABLES

CHAPTER ONE
Introduction

CIRCADIAN RHYTHMS

Properties of circadian rhythms

Circadian [from Latin circa about + diēs day] rhythms are intrinsic biochemical, physiological, and behavioral processes that occur at about 24-hour intervals. These rhythms persist under constant conditions but are also adjusted by external cues such as light, thus allowing an organism to adapt its internal state to the environment. The proper functioning and adjustment of circadian rhythms are thought to be critical for the fitness and health of an organism. There is now a growing realization that the disruption of circadian rhythms in humans, seen for example in night-shift workers and in jet lag, lead not only to sleep disorders but also to increased risks of health detriments such as cancer, metabolic syndrome, cardiovascular disorders, and psychiatric illnesses (Hastings et al., 2003; Takahashi et al., 2008). This thesis addresses mechanisms underlying the generation of circadian rhythms in the suprachiasmatic nuclei (SCN), also known as the master circadian clock.

The intracellular molecular clock

Intracellularly, multiple negative feedback loops form the molecular basis of circadian rhythms within rhythmic cells of the SCN and peripheral tissues. The transcription factors, CLOCK and BMAL1, heterodimerize to drive the expression of *Period* (*Per1*, *2*, and *3*) and *Cryptochrome* (*Cry1* and *Cry2*), which in turn feedback inhibit its own transcription by CLOCK and BMAL1. This inhibition is slowly relieved as PER and CRY are degraded

by the 26S proteasome pathway through association with specific ubiquitin ligase complexes. The F-box proteins, βTrCP1 and βTrCP2 have been shown to regulate the ubiquitination of PERs (Eide et al., 2005; Ohsaki et al., 2008; Shirogane et al., 2005) while FBXL3 and FBXL21 are involved in the ubiquitination of CRYs (Godinho et al., 2007; Hirano et al., 2013; Siepka et al., 2007; Yoo et al., 2013). Additionally, a second transcriptional feedback loop involving *Rev-erbα* and *retinoid-related orphan receptor-α* (*RORα*) modulate the expression of *Bmal1*(Cho et al., 2012; Preitner et al., 2002; Sato et al., 2004; Triqueneaux et al., 2004). These interconnected feedback loops, along with other levels of regulation such as post-translational modification and nuclear translocation of clock gene products, generate a robust near 24 hour rhythm that drives the oscillation of a large variety of different output genes. Disruption of components of these interconnected processes lead to abnormal behavioral circadian rhythms.

The suprachiasmatic nuclei is the master circadian pacemaker in mammals

In mammals, circadian rhythms are controlled centrally by the SCN, located within the anterior hypothalamus (Welsh et al., 2010). Complete lesions of the SCN causes the loss of coordinated daily behavioral circadian rhythms in rodents (Moore and Eichler, 1972; Stephan and Zucker, 1972). Critically, SCN transplants restore the rhythms of the SCN-lesioned host with the period of the donor animal (Ralph et al., 1990; Sujino et al., 2003). Altogether, these key studies established that the SCN is both required and sufficient for the generation of circadian rhythms in behavior.

Structure and regional function of the SCN

The SCN can be divided into the ventral "core" and the dorsal "shell" based on anatomical and functional differences (Abrahamson and Moore, 2001; Morin et al., 2006; Welsh et al., 2010). A less functionally characterized "central" region of the SCN is also anatomically identifiable by neuropeptide markers. The core region of the SCN, which is marked by the presence of vasoactive intestinal polypeptide (VIP), sits adjacent to the optic chiasm and receives direct light input from the retina via the retinohypothalamic tract. The shell region of the SCN, characterized by the expression of arginine vasopressin (AVP), surrounds the core and receives light-induced signals indirectly via projections from the core (Abrahamson and Moore, 2001). Functional heterogeneity between the core and the shell can be readily observed in the different resetting response of the two regions by light stimuli. For proper anticipation of the day/night cycle, the SCN must adjust or entrain to the 24-hour daily cycle by daily "phase-shifts" in response to ambient light signals. Following a phase-shifting light pulse, acute induction of the light-responsive clock genes *Per1* and *Per2* occur rapidly only in the retinorecipient core but not in the shell (Yan and Silver, 2002; Yan et al., 1999). Similarly, light induction of immediate early genes such as *c-Fos, FosB*, and *Fra-2* are also limited to the core (Kornhauser et al., 1990, 1992; Schwartz et al., 2000).

Under constant darkness without light stimuli, functional differences between the core and the shell have also been seen. In contrast to the pattern of *Period* expression after light exposure, it was observed that in constant darkness, *Per1* and *Per2* rhythmic expression *in vivo* begins in the shell then gradually spreads ventrolaterally towards the core (Hamada et al., 2004). *In vitro* studies using *Period* promoter-driven fluorescent or bioluminescent

reporters have also shown that cell populations in the shell appear to phase lead the ones in the core (Yamaguchi et al., 2003). In addition to this difference in phase relationship, the expression or the amplitude of PER oscillation is also much more prominent in the shell than in the core, where it is detected only by more sensitive in vitro methods (Karatsoreos et al., 2004; Shigeyoshi et al., 1997; Welsh et al., 2010). These differences between the core and shell regions of the SCN highlight the functional heterogeneity of different populations of SCN cells.

Intercellular communication in the SCN

The SCN contain heterogenous population of cells characterized by different neurotransmitters and neuropeptides that are expressed in distinct regions within the SCN. Recent screens have identified more than 100 secreted factors produced by SCN cells including neuropeptide precursors, cytokines, and growth factors (Lee et al., 2010). These include somatostatin, angiontensin II, enkephalin, cholecystokinin, neurotensin, and the three most well known neuropeptides in the SCN: vasoactive intestinal peptide (VIP), arginin vasopressin (AVP), and gastrin-releasing peptide (GRP). These neuropeptides, along with another less characterized neuropeptide called neuromedin S (NMS) will be briefly discussed here.

Vasoactive intestinal peptide (VIP)

Produced by neurons located in the core, VIP is one of the most influential intercellular signals within the SCN. Mutant mice lacking VIP or its $VPAC_2$ receptor exhibit

low levels of rhythmic clock gene expression and weak behavioral rhythms (Colwell et al., 2003; Harmar et al., 2002). Transgenic mice overexpressing the receptor for VIP, $VPAC_2$, also have abnormal circadian phenotypes both in response to light stimuli and in constant darkness (Shen et al., 2000). VIP has been shown to induce calcium influx, elicit changes in neuronal firing rate, and shift the phase of the SCN (An et al., 2011; Reed et al., 2001). VIP also plays a prominent role in synchronization between SCN cells. The cells of VIP-deficient SCN fail to synchronize their daily rhythms in molecular gene oscillation (Maywood et al., 2006a). Altogether, these studies demonstrate the critical role of VIP signaling within the SCN. Besides VIP, however, other neuropeptides such as GRP and AVP also play a part in intercellular communication within the SCN.

Gastrin-releasing peptide (GRP)

Found in the central region of the SCN, GRP-expressing neurons, like VIP-positive cells in the core, also receive retinal input and respond to nocturnal light with increased transcription of the immediate early genes (Karatsoreos et al., 2004). Mice lacking the GRP receptor has been shown to exhibit attenuated shifts to bright light (Aida et al., 2002). Application of GRP in vivo can also shift the rhythms of the SCN (Kallingal and Mintz, 2007) and restore coordinated circadian rhythms in SCN deficient in VIP signaling (Maywood et al., 2011).

Arginine vasopressin (AVP)

Synthesized by neurons located in the shell region of the SCN, AVP can also act as a synchronizing agent when VIP signaling is compromised (Maywood et al., 2011). Mice deficient for the V1a receptor, a receptor for AVP, display mostly normal periodicity, but a small percentage of mice exhibit disrupted daily rhythms (Li et al., 2009), supporting a functional role for AVP in intercellular signaling.

Neuromedin S (NMS)

NMS, originally isolated as a ligand for neuromedin U receptors from rat brain extracts, is neuropeptide that is highly selectively expressed in the SCN (Mori et al., 2005). Although mice deficient in NMS exhibit normal free-running periods (Alex et al., 2010), the *in vivo* application of NMS has been shown to induce non-photic type of phase shifts in the locomotor circadian rhythm (Mori et al., 2005). The role of NMS in intercellular communication remains to be elucidated.

Output pathways of the SCN

From the SCN, time-related information must be projected out of the SCN to control the rhythms of other brain areas and the peripheral tissues. The SCN projects to three main areas: the hypothalamus, the thalamus, and the septal area (Leak and Moore, 2001; Leak et al., 1999). The core SCN sends efferent outputs mainly to the shell, the lateral subparaventricular zone, and hypothalamic areas near the vicinity of the SCN. The shell SCN projects more widely to various areas of the brain, particularly the paraventricular nucleus of the thalamus, the paraventricular nucleus of hypothalamus, the medial

subparaventricular zone, the preoptic area, and the dorsomedial hypothalmic nuclei (Leak and Moore, 2001; Leak et al., 1999).

CHAPTER TWO
Methodology

MATERIALS AND METHODS

Mouse breeding

The generation of *Nms-iCre, tetO-Clock*$^{\Delta 19}$, and *tetO-Per2* trangenic lines were described previously (Chang et al., 2010; Chen et al., 20009; Hong et al., 2007). Homozygous ROSA26-lox-stop-lox-tTA mutant mice were obtained from JAX (Wang et al., 2008) and hemizygous transgenic TeNT mice were provided by RIKEN (Yamamoto et al., 2003). To generate experimental mice efficiently, hemizygous *Nms-iCre* mice were crossed with ROSA26-lox-stop-lox-tTA mice for two generations to generate mice that are hemizygous for *Nms-iCre* and homozygous for ROSA26-lox-stop-lox-tTA (referred to as *R26-Nms*). Likewise, the hemizygous *tetO-* lines (*tetO-Clock*$^{\Delta 19}$, *tetO-Per2*, and *tetO-TeNT*) were also bred individually with ROSA26-lox-stop-lox-tTA mice for two generations to generate mice that are hemizygous for the *tetO-* transgene and homozygous for ROSA26-lox-stop-lox-tTA (referred to as *R26-Clock*$^{\Delta 19}$, *R26-Per2*, and *R26-TeNT*, respectively). Subsequently, *R26*-NMS mice were crossed with *R26-Clock*$^{\Delta 19}$, *R26-Per2*, or *R26-TeNT* to generate mice that express the *Clock*$^{\Delta 19}$, *Per2*, or TeNT transgene, respectively, under the regulation of ROSA26-driven tTA in *Nms*-expressing neurons. For simplicity, these quadruple transgenic mice are referred to as *Nms-Clock*$^{\Delta 19}$, *Nms-Per2*, or *Nms-TeNT*. Control mice that lack either the *Nms-iCre* and/or the *tetO-* transgene are also produced from these crosses. For bioluminescence experiments, PER2::LUC mice (Yoo et al., 2004) were crossed with ROSA26-lox-stop-lox-tTA for at least two generations to produce mice

homozygous for both alleles. Subsequently, these mice are crossed with *Nms-Clock*$^{\Delta 19}$, *Nms-Per2*, or *Nms-TeNT* to generate mice that carry a hemizygous copy of *Nms-iCre*, a homozygous copy of ROSA26-lox-stop-lox-tTA, a heterozygous copy of PER2::LUC, and a hemizygous copy of either the *Clock*$^{\Delta 19}$, *Per2*, or TeNT transgene. All experimental mice used were backcrossed to C57B6/J for at least 5 generations.

Dox treatment

Doxycycline hyclate (Sigma-Aldrich; D9891) was given ad libitum in drinking water at a concentration of 10 μg/ml or 20 μg/ml as stated and renewed every 3 to 4 days (Hong et al., 2007). All mice were given free access to regular food.

Circadian behavioral recording and analyses

Running wheel activity of singly housed mice was recorded by ClockLab (Actimetrics) as described previously (Siepka and Takahashi, 2005). All mice used were adults at least 8 weeks of age. Mice were entrained to a light/dark (LD) 12:12 cycle for a minimum of 7 days prior to release into constant darkness. Free-running period was calculated by χ^2 periodogram using the 21 days right before a change in condition (water vs. Dox; light vs. dark) or before the end of experimentation. Fast Fourier transform was used to calculate the relative power of the circadian component from 18-30 hours. Losses of circadian rhythms were assessed based on visual inspection of the activity record in conjunction with FFT and χ^2 periodogram analysis (Low-Zeddies and Takahashi, 2001).

Animals with a loss of circadian rhythms were excluded from period calculations. All values are displayed as the mean ± the standard error of the mean (SEM).

Immunohistochemistry

Mice were anesthetized with ketamine/xylazine/saline cocktail (ketamine, 10 mg/ml; xylazine, 2 mg/ml) at 0.01 ml/g and intracardially perfused with 5-10 ml of 0.9% saline solution followed by 50 ml of 4% paraformaldehyde (Sigma-Aldrich) in PBS, pH 7.4. Brains were removed and postfixed overnight at 4°C in 4% paraformaldehyde. Coronal sections (50 μm thick) were prepared using a Vibratome (Leica Microsystems). Free-floating sections were blocked in 3% normal goat serum (Vector Laboratories) with phosphate-buffered saline (PBS; pH 7.4) containing 0.3% Triton X-100 at room temperature for 1 h, followed by incubation with primary antibodies in PBS + 3% normal goat serum and 0.3% Triton X-100. After 2 overnight incubation of primary antibodies in 4°C, sections were washed 3 times with PBS and stained with the appropriate secondary antibodies in PBS + 0.3% Triton X-100 at room temperature for 1 h. Following this, sections were washed with PBS 3 times and incubated with ToPRO-3 1:100 (Invitrogen) at room temperature for 1 h. For stereological counting, sections were incubated with NeuroTrace® 530 Red Fluorescent Nissl Stain 1:100 (Invitrogen). After staining, all sections were washed and mounted with ProLong® Gold Antifade Reagent with DAPI (Invitrogen).

Primary antibodies used were rat anti-HA 1:100 (Roche), chicken anti-GFP 1:500 (Invitrogen), rabbit anti-NMS 1:1000 (Bachem), guinea pig anti-VIP 1:2000 (Phoenix Pharmaceuticals), rabbit anti-AVP 1:4000 (Immunostar), rabbit anti-GRP 1:500

(Immunostar), and guinea pig anti-PER2 1:2000 (Yoo et al., 2013). Secondary antibodies include goat anti-rat Alexa 488 1:500 (Invitrogen), goat anti-chicken Alexa 488 1:500 (Invitrogen), goat anti-rabbit Alexa 488 1:500 (Invitrogen), goat anti-rabbit Alexa 546 1:500 (Invitrogen), and goat anti-guinea pig Alexa 546 1:500 (Invitrogen).

Imaging data collection

Fluorescence-immunolabeled images were acquired using a Zeiss LSM 510 confocal microscrope without any post-processing. ImageJ was used for co-localization analyses using images taken at 20X.

Stereological cell counting

Fluorescent staining was visualized and subjected to stereological analysis using a Olympus BX-51 microscope and Stereo Investigator software (MBF Bioscience). Every other SCN coronal sections (50 μm) from one brain hemisphere were counted from anterior to posterior with an unbiased counting frame according to the optical dissector principle. A grid size of 80 x 80 and a frame size of 25 x 25 were used for anti-HA and anti-TeNT stained slices. For NeuroTrace Nissl staining, a grid size of 60 x 60 and a frame size of 20 x20 were used. All contours were drawn at 10X magnification and counted at 100X magnification. Approximately 200 cells were counted for each brain series. In all samples, the coefficient of error (CE, Gundersen m=0), a measure of the precision of stereological estimates (Gundersen and Jensen, 1987), ranged from 0.08 – 0.11.

Explant culture and bioluminescence data analysis

All mice used were adults at least 8 weeks of age. Following methods described previously (Yamazaki and Takahashi, 2005; Yoo et al., 2004), after cervical dislocation, the brain was removed and placed immediately in Hank balanced salt solution (HBSS; with 10 mM HEPES, 25 units/ml penicillin, and 25 ug/ml streptomycin) on ice. Coronal slices containing the SCN were sectioned at 300 μm using a vibrotome, followed by manual dissection of the SCN, resulting in a tissue approximately 1 mm by 1 mm in size. Dissected SCN tissues were cultured on a Millicell culture membrane (PICMORG50, Millipore) with 1.2 ml DMEM medium (Cellgro), supplemented with 10 mM HEPES (pH 7.2), 2% B27 (Invitrogen), 25 units/ml penicillin, 25 mg/ml streptomycin, and 0.1 mM luciferin (Promega). Explant cultures were maintained at 36°C in an incubator or in a temperature-controlled room. Bioluminescence was continuously monitored without interruption for >7 d immediately upon placement in culture with LumiCycle photomultiplier tube (PMT) detector systems (Actimetrics, Wilmette, IL).

For bioluminescence analyses, LumiCycle software (Actimetrics) was used to subtract the 24 hours moving average from the raw luminescence data and smoothed by 0.5 h adjacent averaging (Pendergast et al., 2009). To determine the period, baseline-subtracted and smoothed data were exported to ClockLab (Actimetrics) and determined by fitting a regression line to the acrophase of at least 3 days of the PER2::LUC rhythm. To quantitatively assess amplitude, the second peak of the baseline-subtracted, smooth data was assessed. All values are displayed as the mean ± the standard error of the mean (SEM).

CHAPTER THREE
Results

THE ROLE OF NEUROMEDIN S (NMS)-PRODUCING CELLS IN THE SCN

In mammals, circadian rhythms are controlled centrally by the SCN, located within the anterior hypothalamus. Complete lesions of the SCN causes the loss of coordinated daily behavioral circadian rhythms in rodents (Moore and Eichler, 1972; Stephan and Zucker, 1972) while transplants of SCN restore the rhythms of the SCN-lesioned host with the period of the donor animal (Ralph et al., 1990; Sujino et al., 2003). Altogether, these key studies established that the SCN is both required and sufficient for the generation of circadian rhythms in behavior. Within the SCN, however, approximately 20,000 neurons function to synchronously generate coherent outputs in behavior rhythms. Although it has been shown that behavioral circadian output is the result of integration of SCN cellular phenotypes (Low-Zeddies and Takahashi, 2001), it remains unknown whether certain subsets of these cells are required and/or sufficient to exert control over behavioral circadian rhythms. In this dissertation, I describe our combinatorial genetic approaches to ask the question, "Is there a particular subpopulation of neurons that is both required for the generation of circadian rhythms in behavior and sufficient to impose its rhythmic timing among other cellular oscillators within the SCN?"

In order to address this question, we aimed to restrictively target subpopulations of the SCN while minimally affecting other regions of the brain to minimize off-target effects. To this end, we utilized the *Nms-iCre* BAC transgenic mouse line, a novel transgenic line that expresses iCre under the promoter of *neuromedin S* (*Nms*). This mouse line was

partially characterized and described in a dissertation (Chang et al., 2010). Here, we further characterize the mouse line and found that *Nms*-positive neurons represent ~40% of all SCN neurons and is expressed in the majority of VIP- and AVP-positive cells with no detectable expression in GRP-positive cells. Thus, *Nms-iCre*, which we found to express iCre restrictively in *Nms*-positive cells of the SCN, represents a suitable genetic tool to dissect out the cellular roles of subpopulations of the SCN marked by NMS.

First, to determine whether *Nms*-expressing neurons can control the behavioral rhythms of the mouse, we altered the intracellular clock rhythms of *Nms*-positive cells by overexpressing two different circadian genes involved in the core clock machinery, the dominant negative mutant $Clock^{\Delta 19}$ and *Per2*. CLOCK, which dimerizes with BMAL1 to induce the transcription of *Period* and *Cryptochrome*, is a key regulator of the positive limb of the transcriptional-translational feedback loop. The heterozygous $Clock^{\Delta 19}$ mutation results in mice with a lengthened period of ~24.4 hours (Vitaterna et al., 1994). Overexpressing the $Clock^{\Delta 19}$ mutation in >90% of the SCN cells using the *secretogranin II* (*Scg2*) promoter also lead to an one hour longer period (Hong et al., 2007). This was accomplished by crossing the *tetO-*$Clock^{\Delta 19}$ transgenic line with the *Scg2-tTA* transgenic mouse line. PER2, which heterodimerizes with CRY to inhibit the transcription of CLOCK:BMAL1 complexes, is an essential component of the negative limb of the core clock machinery. Constitutive overexpression of PER2 using the *Scg2* promoter (*tetO-Per2* x *Scg2-tTA*) caused a complete loss of behavioral circadian rhythms (Chen et al., 2009a). Using the tetracycline-controlled transactivator (tTA) system, we crossed *tetO-*$Clock^{\Delta 19}$ or *tetO-Per2* with *Nms-iCre* and ROSA26-lox-stop-lox-tTA to generate mice that conditionally

overexpress *Clock*$^{\Delta 19}$ or *Per2*, respectively, in a doxycycline (Dox)-dependent manner. Interestingly, we found that the expression of *tetO-Clock*$^{\Delta 19}$ or *tetO-Per2* only in NMS-positive neurons of the SCN is sufficient to lengthen or abolish the behavioral circadian rhythms of the mice, respectively.

In order to ascertain the role of a population of cells, we must determine the consequences of its absence. Next, to assess whether *Nms*-expressing cells are required for the generation of behavioral circadian rhythms, we utilized tetanus toxin light chain to disrupt its neurotransmission in a Dox-dependent manner. The *tetO-TeNT* transgenic line was crossed with *Nms-iCre* and ROSA26-lox-stop-lox-tTA to generate mice that can reversibly disrupt synaptic neurotransmission in *Nms*-positive neurons. TeNT is a potent zinc protease that specifically cleaves VAMP2 to inhibit evoked neurotransmitter release. Much to our surprise, we found that when TeNT is expressed in *Nms*-positive neurons, circadian rhythms in behavior are abolished, suggesting that *Nms*-producing cells in the SCN are required for the generation of behavioral circadian rhythms. Taken together, our results indicate that *Nms*-expressing neurons have indispensible roles in the production of coherent daily rhythms in behavior.

Results

Nms-iCre transgenic drives *Clock*$^{\Delta 19}$ expression within endogenous *Nms* cells

In order to conditionally overexpress *Clock*$^{\Delta 19}$ in *Nms*-positive cells of the SCN, we crossed the *Nms-iCre* mouse line with the ROSA26-lox-stop-lox-tTA and the *tetO-Clock*$^{\Delta 19}$ transgenic mouse lines (referred to as *Nms-Clock*$^{\Delta 19}$; Figure 1-1; see Methods). To confirm that the *Clock*$^{\Delta 19}$ transgene is expressed in the endogenous *Nms*-expressing cells in *Nms-Clock*$^{\Delta 19}$ mice, we performed double immunohistochemistry using anti-HA and anti-NMS antibodies following ICV treatment with colchicine to strengthen the detection of NMS in the cell soma. Without colchicine treatment, only a very minimal number of NMS-positive cells can be faintly visualized (data not shown). As shown in Figure 1-2, we found a nearly complete overlap between HA and NMS immunoreactivity. Specifically, ~97% of *Clock*$^{\Delta 19}$ overlaps with NMS and ~93% of NMS overlaps with *Clock*$^{\Delta 19}$. Accounting for the detection limitations of the antibodies, we conclude that in the *Nms-Clock*$^{\Delta 19}$ mouse line, the *Clock*$^{\Delta 19}$ transgene is faithfully expressed only in SCN neurons marked by NMS.

Characterization of the number and expression pattern of *Nms* cells within the SCN

NMS was first purified from the rat brain and reported to be expressed in a core-like pattern within the rat SCN (Mori et al., 2005). However, neuropeptide markers such as VIP, which is expressed in the SCN core (Abrahamson and Moore, 2001; Silver et al., 1999) were

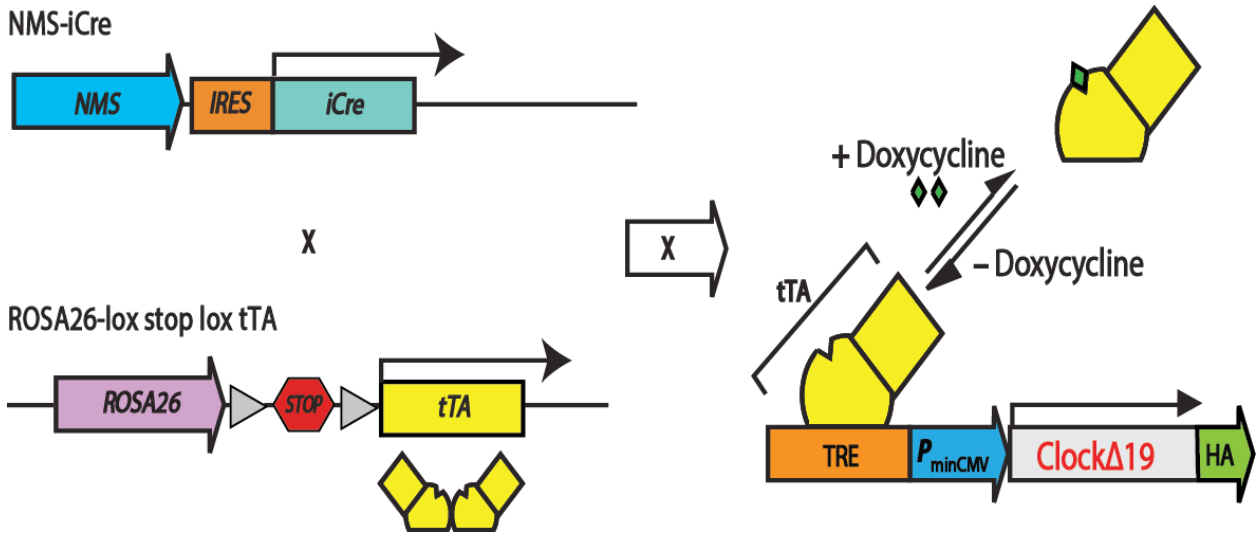

Figure 1-1. Schematic diagram showing the Tet-Off system and constructs used for generating the *Nms-Clock*$^{\Delta 19}$ mice. The *Nms* promoter drives the expression of iCre, which excises the loxP flanked stop codon of ROSA26-lox-stop-lox-tTA, allowing tTA to be expressed. tTA binds to the tetO promoter (also known as the Tetracycline Response Element (TRE)) in the absence of doxycycline (Dox) but not in its presence, resulting in the transcriptional activation or repression of the *Clock*$^{\Delta 19}$ transgene, respectively.

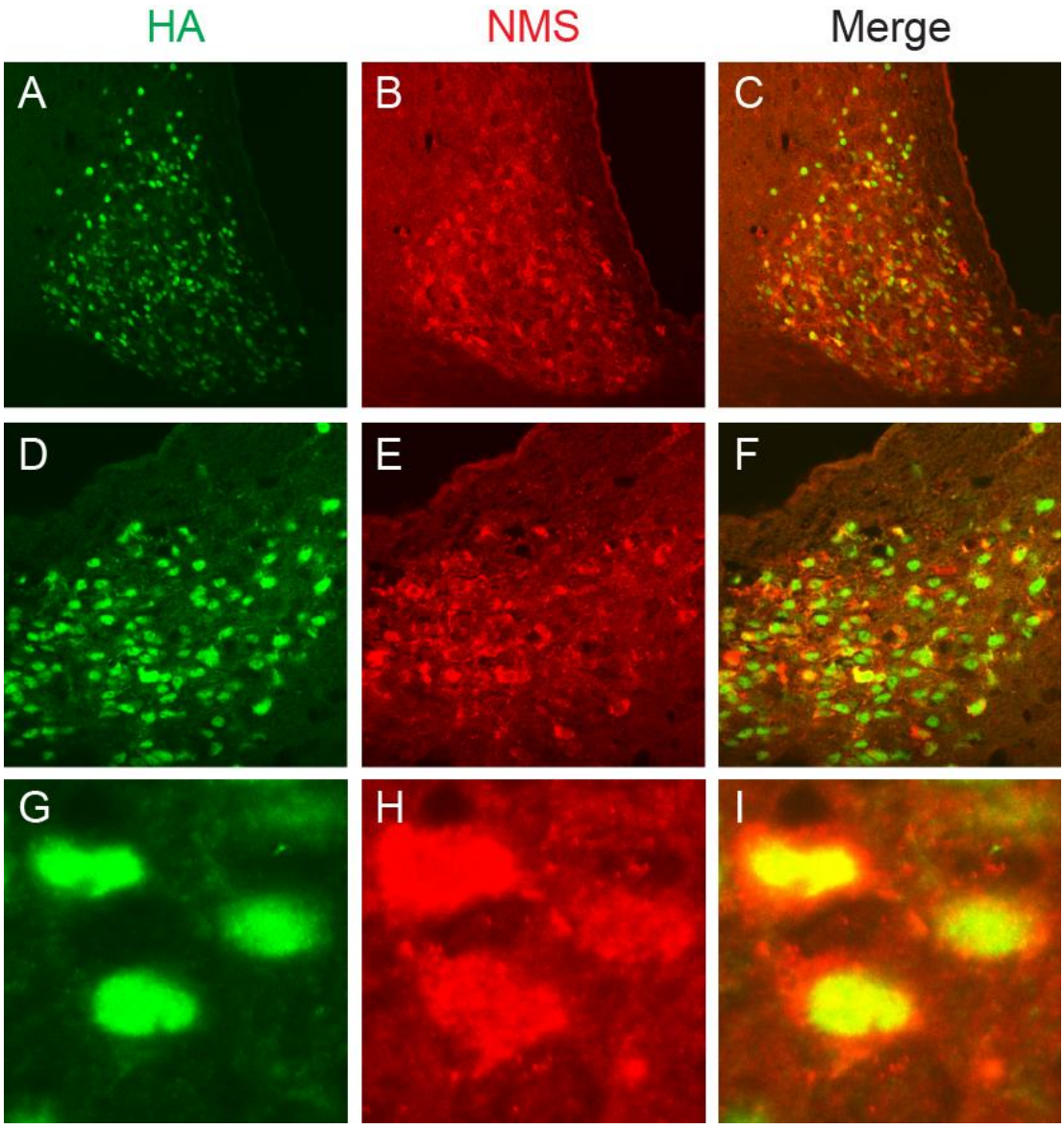

Figure 1-2. *Nms-iCre* drives *Clock*$^{\Delta 19}$ expression within endogenous NMS-positive cells in the SCN. Representative images captured with a 20X (A-C), 40X (D-F), and 63X (G-I) objectives are shown. *Clock*$^{\Delta 19}$ is tagged with an HA epitope. HA overlapped with 93% of NMS-immunoreactive cells while NMS co-localizes with 97% of HA-positive cells.

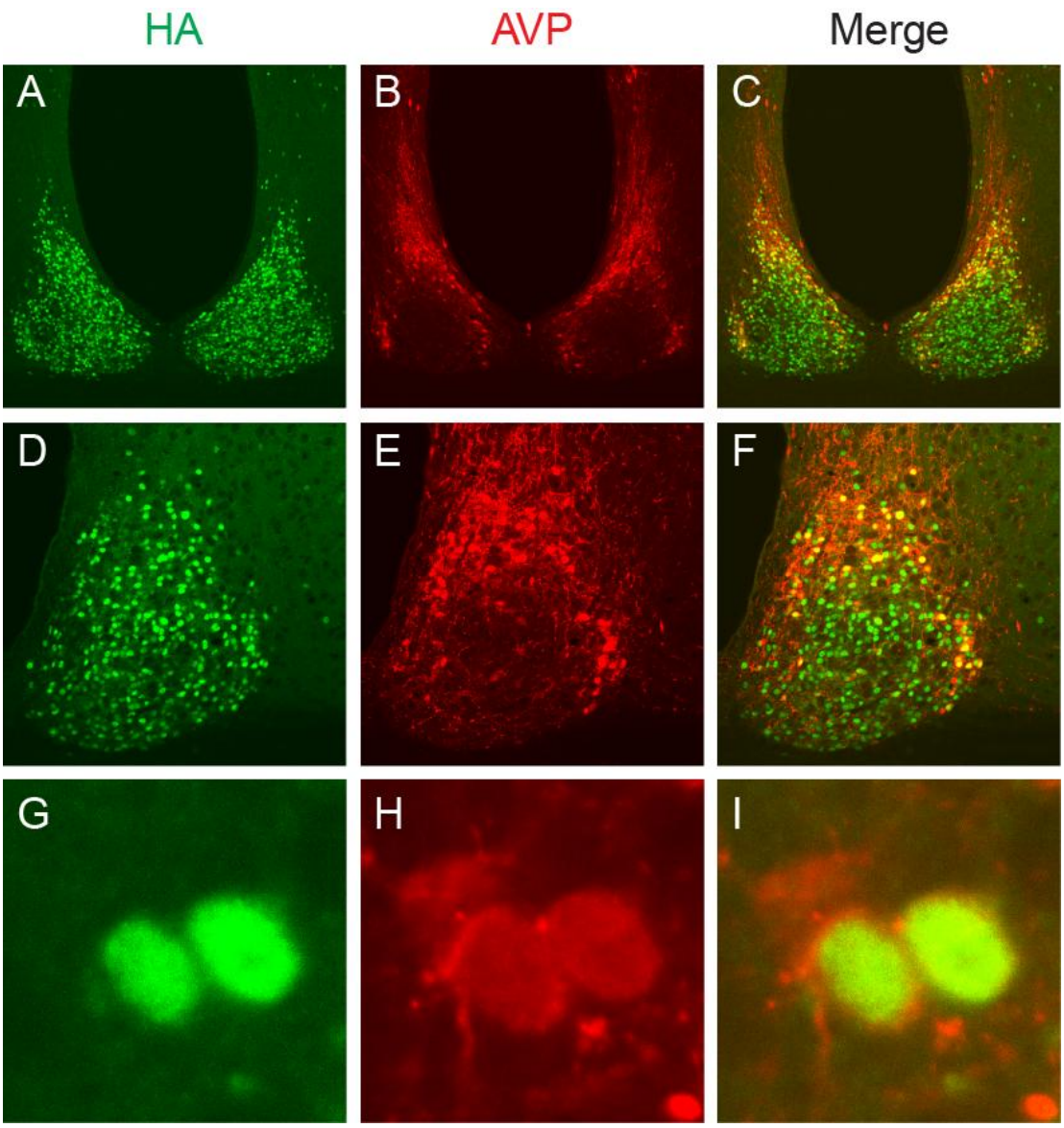

Figure 1-3. HA (*Nms*) co-localization with AVP-expressing cells in the SCN shell. Representative images captured with a 10X (A-C), 20X (D-F), and 63X (G-I) objectives are shown. HA overlapped with 94.7% of AVP-immunoreactive cells, which corresponds to 32.5% of HA-positive NMS-producing cells.

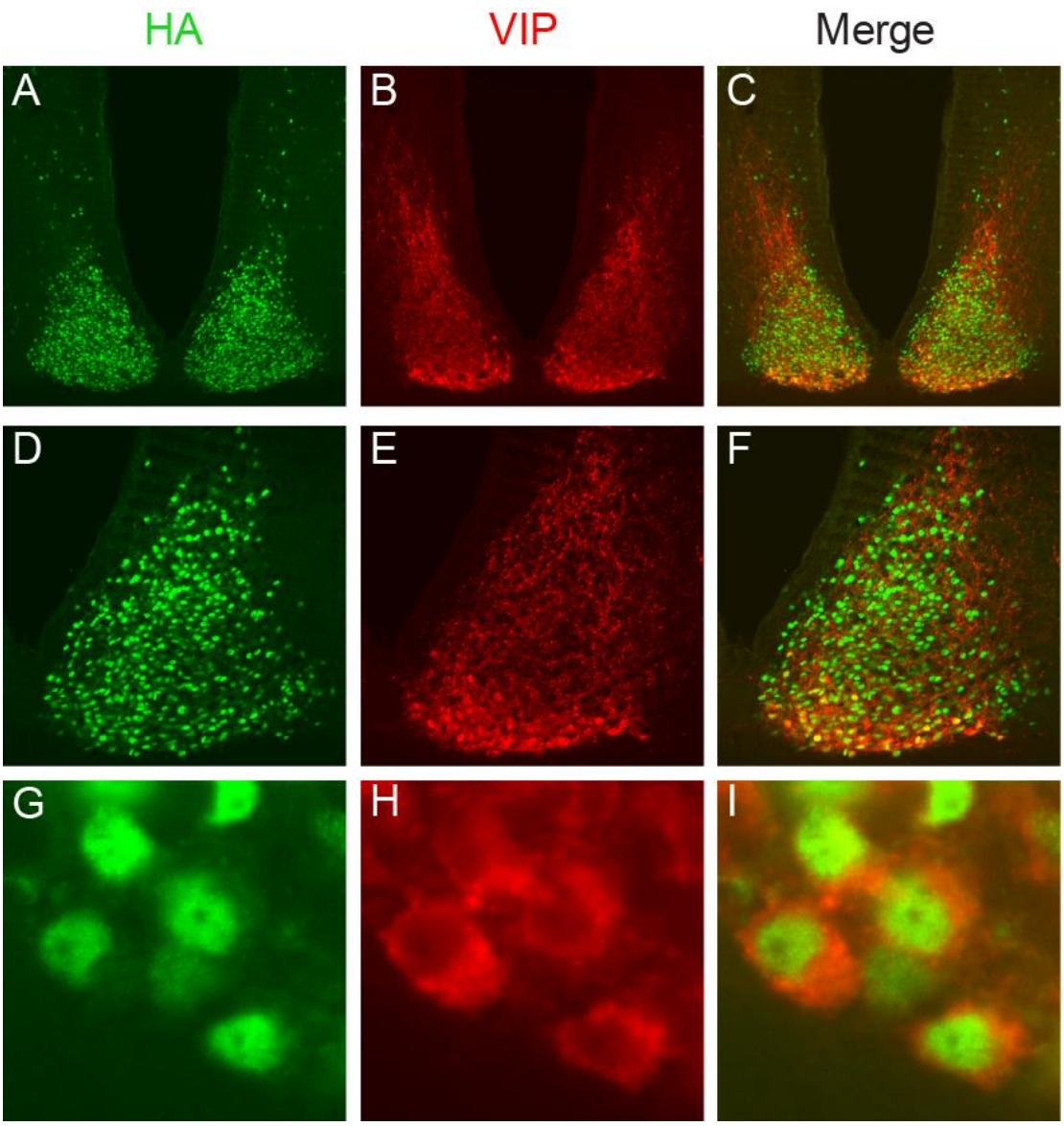

Figure 1-4. HA (*Nms*) co-localization with VIP-expressing cells in the SCN core. Representative images captured with a 10X (A-C), 20X (D-F), and 63X (G-I) objectives are shown. HA overlapped with 95.5% of VIP-immunoreactive cells, which corresponds to 21.8% of HA-positive NMS-producing cells.

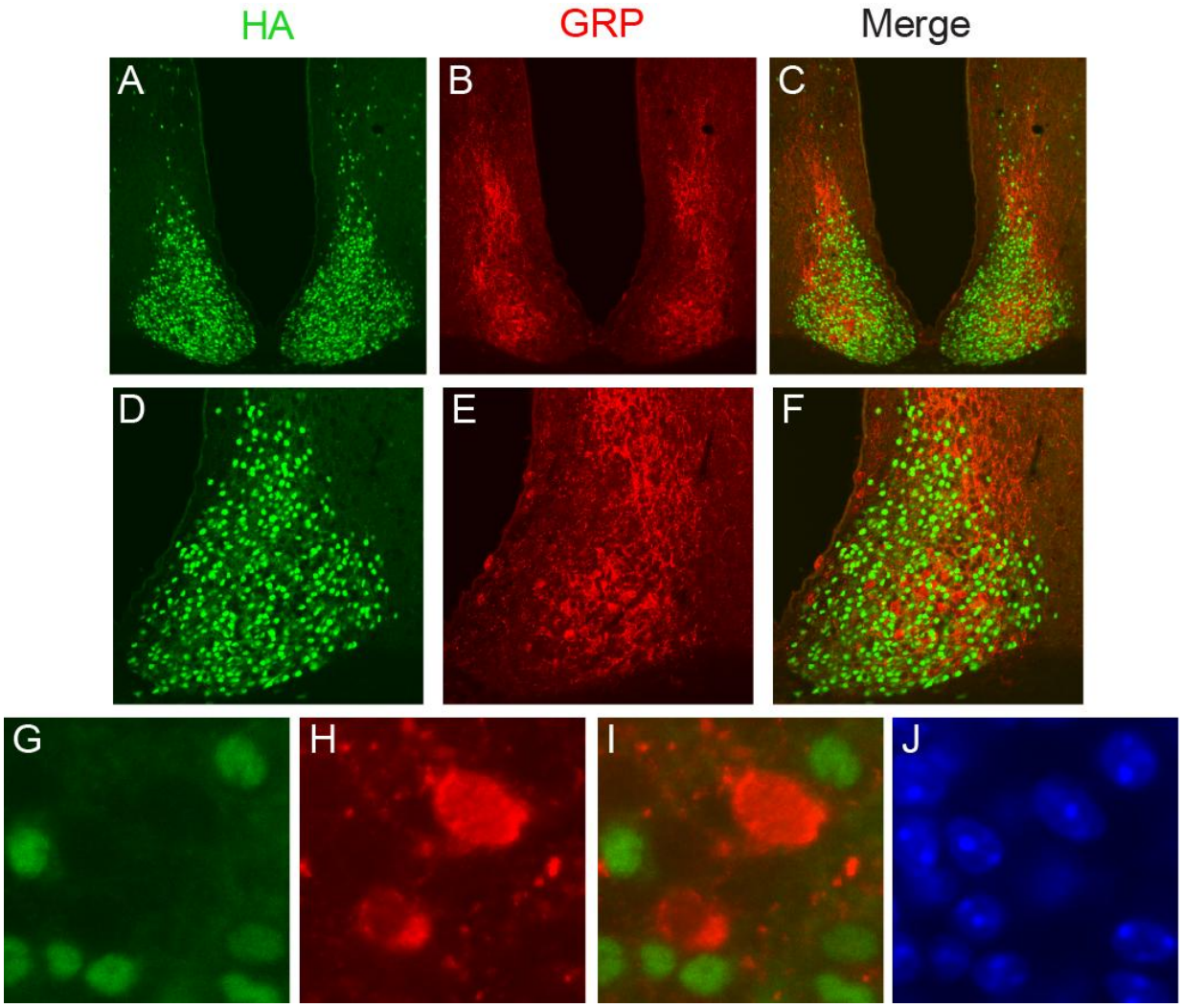

Figure 1-5. HA (*Nms*) does not co-localize with GRP-expressing cells in the SCN. Representative images captured with a 10X (A-C), 20X (D-F), and 63X (G-I) objectives are shown. No overlap was observed between HA and GRP immunoreactivity.

Antibody	Count	Estimated % per SCN
HA	4239±112	40.4%
Nissl	10484±109	

Table 1 . Stereological estimate of *Nms*-expressing neurons in the SCN. Number of *Nms*-expressing neurons are estimated based on stereological counts from one SCN of the brain and represent half of the total cell population. Anti-HA was used for *Nms*-*Clock*$^{\Delta 19}$ (n=3) to estimate the number of *Nms* cells. Nissl staining was used to estimate the total number of neurons. Values are means ± SEM.

not utilized to conclusively determine the localization of NMS in the SCN. Within the mouse SCN, the expression pattern of NMS and the number of SCN cells that express NMS remain uncharacterized. To assess the regional distribution of NMS within the mouse SCN, we used anti-HA to stain for *Nms*-positive neurons in *Nms-Clock*$^{\Delta 19}$ mice. The anti-HA antibody was used in lieu of anti-NMS due to its higher sensitivity towards visualizing *Nms*-expressing cells. As mentioned above, the mouse SCN can be relatively divided into the core and the shell region based on functional and immunohistochemical differences. Neurons in the core and the shell regions of the SCN express VIP and AVP, respectively. A central region of the SCN can also be delineated by the expression of GRP (Morin et al., 2006). To determine the expression of NMS in the core, shell, and central region of the SCN, anti-VIP, anti-AVP, and anti-GRP antibodies were used, respectively, to double stain with an anti-HA antibody. ICV injection of colchicine was used prior to immunohistochemistry using anti-VIP and anti-GRP to increase immunoreactivity in the cell body. As shown in Figures 1-3 and 1-4, a vast majority of AVP- and VIP-expressing neurons are co-labeled with NMS-positive neurons as indicated by HA immunoreactivity. Specifically, HA overlaps with ~94.7% of AVP-immunoreactive cells and ~95.5% of VIP-immunoreactive cells, while AVP and VIP overlap with ~32.5% and ~21.8% of HA-immunoreactive cells, respectively. In contrast, no GRP-expressing neurons were found to overlap with NMS-expressing cells (Figure 1-5).

Next, we utilized unbiased stereological counting (West et al., 1993) to estimate the number of NMS-expressing neurons. To estimate the total number of neurons in the SCN, NeuroTrace Nissl staining was used. As shown in Table 1, the number of estimated total

neurons, ~10,500 neurons per unilateral SCN, correspond well with those reported by other groups (Abrahamson and Moore, 2001; Atkins et al., 2010). The number of *Nms*-expressing cells was estimated to be around ~40% by anti-HA staining. Compared to the estimated number of VIP (~10-22%), AVP (~20%), and GRP (~4-10%) in the SCN (Abrahamson and Moore, 2001; Atkins et al., 2010), NMS appears to be expressed in a much greater numbers of cells. However, direct comparisons of the cell numbers cannot be readily made due to differences in immunohistochemical conditions and counting procedures.

Clock$^{\Delta 19}$ transgenic overexpression is inducible and reversible in *Nms-Clock*$^{\Delta 19}$ mice

In the *Nms-Clock*$^{\Delta 19}$ mice, the *tetO-Clock*$^{\Delta 19}$ transgene is controlled transcriptionally by the ROSA26 promoter-regulated tTA in *Nms*-producing cells of the SCN. The tTA (Tet-Off) system allows for conditional regulation of the transgene expression by doxycycline (Dox) administration. To determine whether the *Clock*$^{\Delta 19}$ transgene can be turned off, 10 μg/ml of Dox in water was given ad libitum for 7 days prior to immunohistochemistry with an anti-HA antibody. By day 7, the CLOCK$^{\Delta 19}$-HA protein was nearly undetectable (Figure 1-6). The water-administered *Nms-Clock*$^{\Delta 19}$ mice exhibit high levels of transgene expression while the control *R26-Clock*$^{\Delta 19}$ mice had no detectable expression. Therefore, in the *Nms-Clock*$^{\Delta 19}$ mice, the *Clock*$^{\Delta 19}$ transgene can be conditionally controlled by Dox.

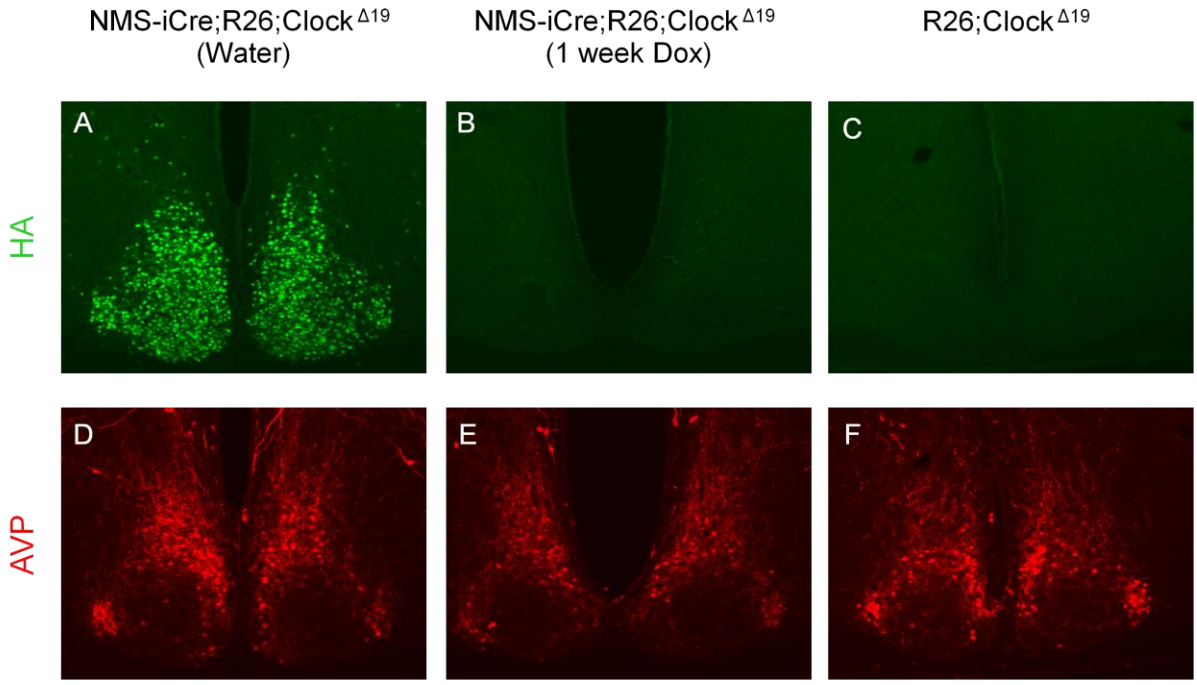

Figure 1-6. The *Clock* $^{\Delta 19}$ transgene can be reversibly expressed in *Nms*-positive neurons of the SCN. Representative images captured with a 10X objective are shown. The SCN of water-administered *Nms-Clock*$^{\Delta 19}$ (A and D), Dox-administered *Nms-Clock*$^{\Delta 19}$ SCN (B and E), and water-administered *R26-Clock*$^{\Delta 19}$ mice (C and E) were stained with anti-HA and anti-AVP. One week of Dox nearly turned off all HA expression in *Nms-Clock*$^{\Delta 19}$ mice.

Nms-Clock$^{\Delta 19}$ mice exhibit long circadian periods in behavioral rhythms

Locomoter wheel running activity was recorded to assess the behavioral circadian rhythms of *Nms-Clock*$^{\Delta 19}$ mice along with littermate controls. Control mice contain the homozygous ROSA26-lox-stop-lox-tTA loci but lack either the *Nms-iCre* transgene (referred to as *R26-Clock*$^{\Delta 19}$), the *tetO-Clock*$^{\Delta 19}$ transgene (referred to as *R26-Nms*), or both transgenes (referred to as *R26*). All mice entrained to light/dark (LD) 12:12 cycle, exhibiting primarily nocturnal activity (Figure 1-7). Upon release into constant darkness (DD), however, *Nms-Clock*$^{\Delta 19}$ mice displayed a lengthened circadian period approximately 1 hour longer than the three control groups of mice (Figures 1-7, 1-8, and 1-9; 24.68 hours vs. ~23.63 hr, respectively; $P<0.05$, two-way ANOVA). To examine whether this lengthened period is dependent on the expression of the *Clock*$^{\Delta 19}$ transgene, 10 μg/ml of doxycycline (Dox) was given *ad libitum* in drinking water to turn off the transgene's expression. Upon Dox administration, control mice continued to run with an unaltered circadian period, while *Nms-Clock*$^{\Delta 19}$ mice displayed a rapid reversal of the lengthened period to a mean circadian period of 23.72 hours, a period length comparable with the control mice. Therefore, the conditional expression of the dominant negative *Clock*$^{\Delta 19}$ transgene in *Nms*-expressing cells in the SCN is sufficient to lengthen the daily rhythms in running wheel activity.

Nms-Clock$^{\Delta 19}$ SCN has long PER2::LUC rhythms

To examine the cellular and molecular effects of *Clock*$^{\Delta 19}$ transgene expression in *Nms*-producing cells of the SCN, we crossed *Nms-Clock*$^{\Delta 19}$ with mice carrying both

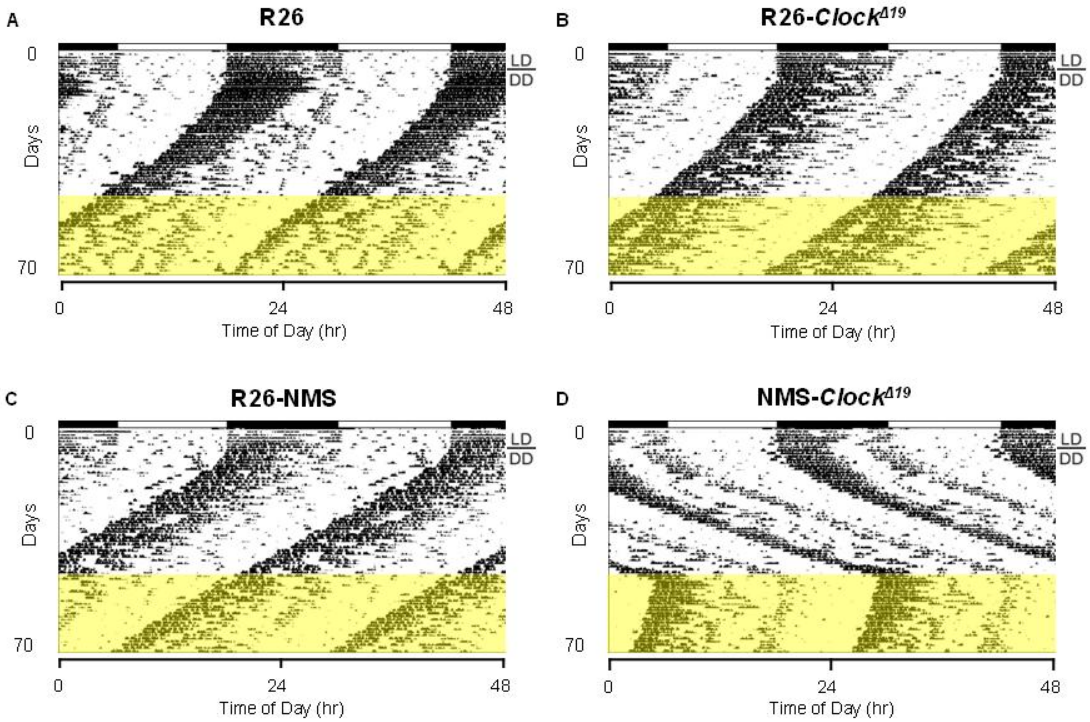

Figure 1-7. Locomotor activity records of *Nms-Clock*$^{\Delta 19}$ transgenic and littermate controls. Representative actograms of A) *R26*; B) *R26-Clock*$^{\Delta 19}$; C) *R26- Nms*; and D) *Nms-Clock*$^{\Delta 19}$ mice. Activity records are double plotted such that 48 hours are represented horizontally, with each day presented below and to the right of the preceding day. The initial light cycle is depicted at the top of the record. All mice were initially placed on a light/dark cycle (LD 12:12) for a minimum of 7 days then transferred into constant darkness (DD), as indicated on the actogram. All *Nms-Clock*$^{\Delta 19}$ mice displayed a lengthening of free-running period of approximately 1 hour. Control mice that lack either *Nms-iCre* and/or *Clock*$^{\Delta 19}$ showed normal free-running periods. Upon switching to Dox water (highlighted in yellow), the period of *Nms-Clock*$^{\Delta 19}$ mice returns to a normal range while control mice exhibit no significant changes in free-running period.

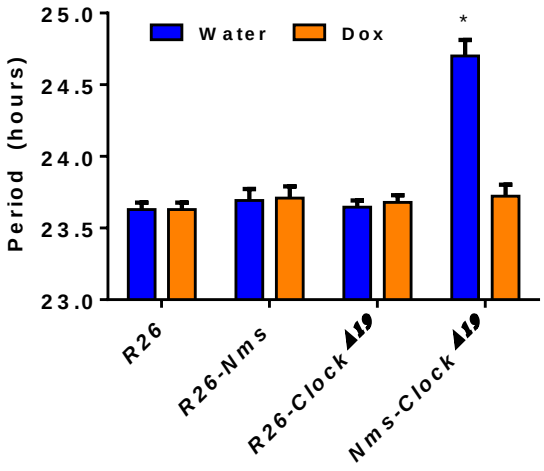

Figure 1-8. Quantification of circadian activity in *Nms-Clock*$^{\Delta 19}$ transgenic and littermate controls. Average free-running period was calculated for all mice. Values are presented as mean ± SEM. No significant differences in mean circadian period were found in controls and Dox-administered *Nms-Clock*$^{\Delta 19}$ mice, while a significantly longer free-running period was observed in water-treated *Nms-Clock*$^{\Delta 19}$ mice compared to the controls ($p < 0.05$ for each comparison). *R26*, n=7; *R26-Nms*, n=6; *R26-Clock*$^{\Delta 19}$, n=12; *Nms-Clock*$^{\Delta 19}$, n=7.

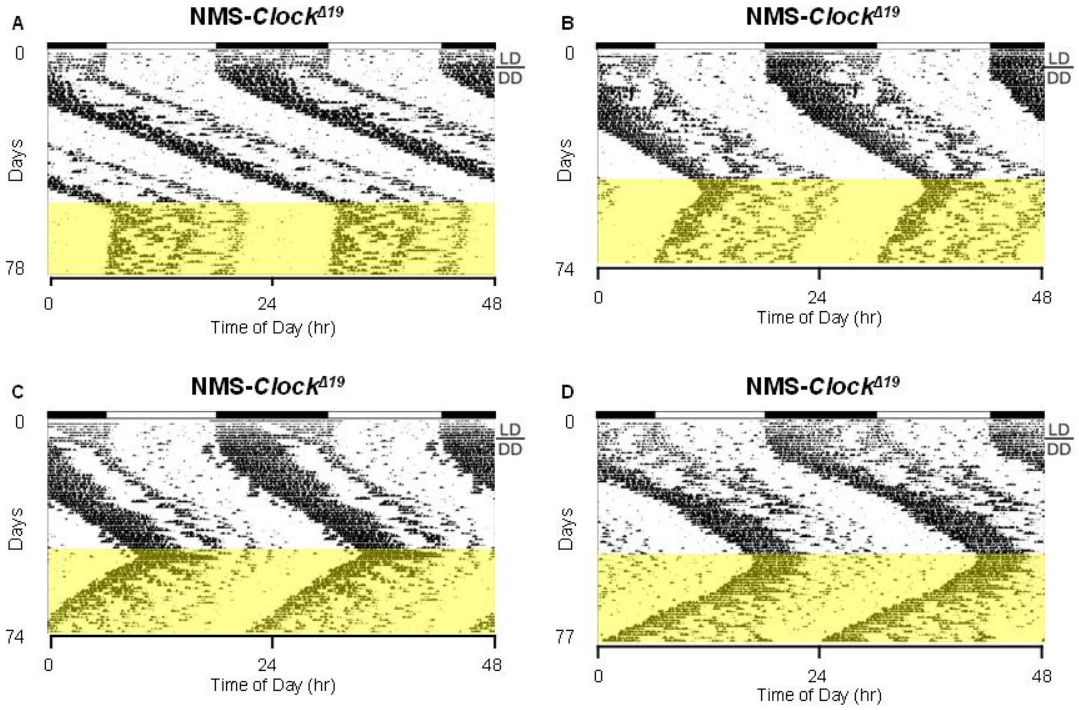

Figure 1-9. More representative locomotor activity records of *Nms-Clock*$^{\Delta 19}$ transgenic mice. Times of Dox administration are highlighted in yellow.

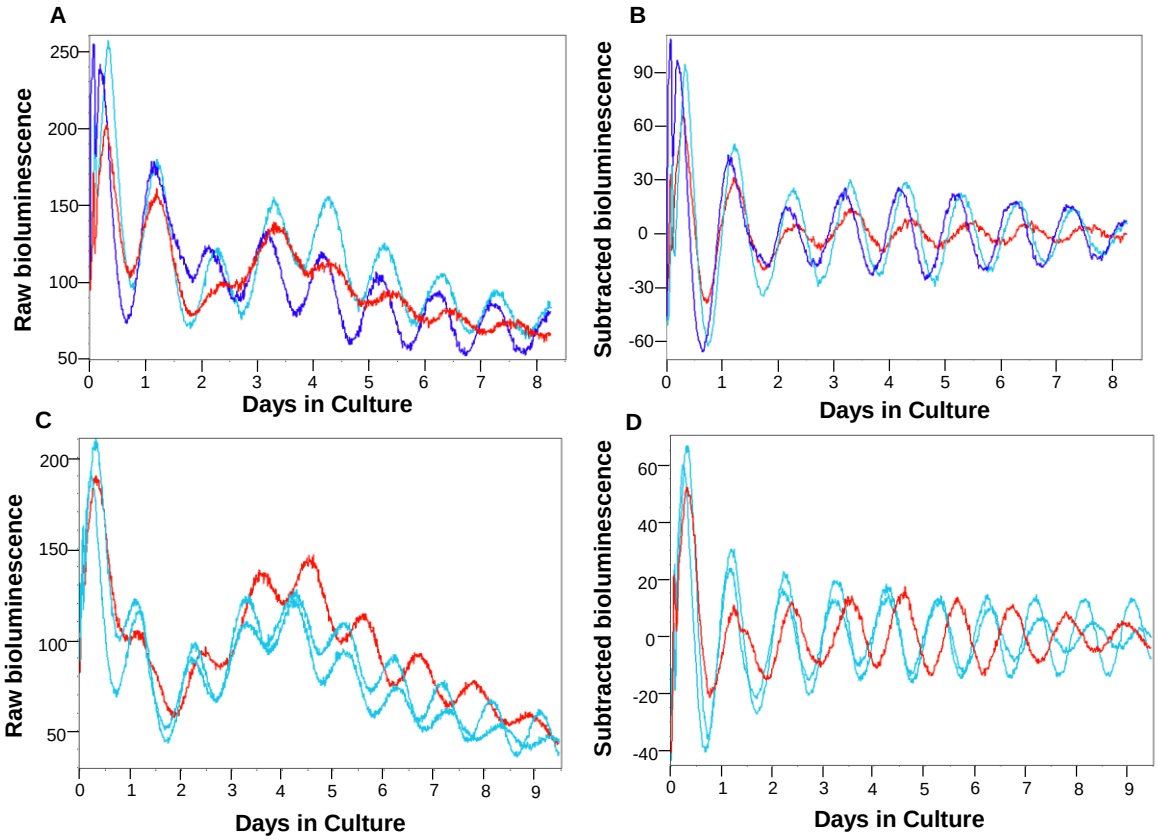

Figure 1-10. Representative bioluminescence records showing PER2::LUC rhythms from the SCN of *Nms-Clock*$^{\Delta 19}$ mice and littermate controls Raw (A and C) and baseline-subtracted (B and D) plots of the SCN of *R26-Nms* (light blue trace), *R26-Clock*$^{\Delta 19}$ (dark blue trace), and *Nms-Clock*$^{\Delta 19}$ (red trace) are shown. The SCN of *Nms-Clock*$^{\Delta 19}$ mice have a longer period compared to the SCN of littermate controls.

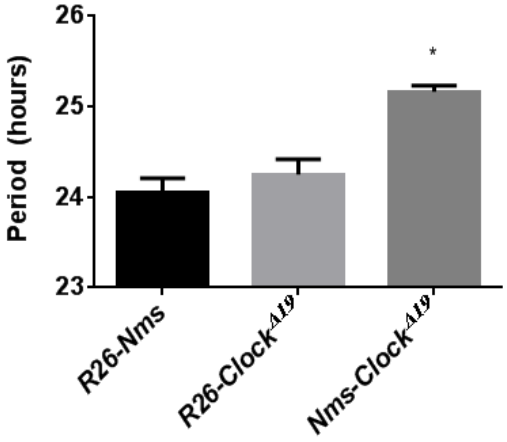

Figure 1-11. Quantification of PER2::LUC period in *Nms-Clock*$^{\Delta 19}$ transgenic and littermate controls. Values are presented as mean ± SEM. The SCN of *Nms-Clock*$^{\Delta 19}$ mice exhibited significantly longer PER2::LUC rhythms compared to controls ($p < 0.05$ for each comparison). No significant differences in mean circadian period were found in controls. *R26-Clock*$^{\Delta 19}$, n=12; *R26-Nms*, n=9; *Nms-Clock*$^{\Delta 19}$, n=8.

ROSA26-lox-stop-lox-tTA and PER2::LUC (see Methods). SCN organotypic cultures from *Nms-Clock*$^{\Delta 19}$ mice expressed robust and rhythmic bioluminescence with a period longer than those of control SCN (Figures 1-10 and 1-11). Since NMS is expressed in ~40% of the entire SCN, these results indicate that the PER2::LUC rhythms of non-*Nms* cells had also likely become longer, since the bioluminescence measurement is taken from the average of the whole SCN explants.

Per2 transgenic overexpression is inducible and reversible in *Nms-Per2* mice

The constitutive overexpression of *Per2* has been shown to abolish circadian rhythms at a cellular and organismal level (Chen et al., 2009b). To determine the behavioral consequences of stopping the molecular rhythms of *Nms*-producing cells within the SCN, we crossed *Nms-iCre* with ROSA26-lox-stop-lox-tTA and *tetO-Per2* transgenic mouse lines (*Nms-Per2*; Figure 2-1; see Methods). First, to validate that the *Per2* transgene can be overexpressed in a reversible manner, water-maintained and Dox-administered *Nms-Per2* mice along with *R26-Per2* control mice were immunostained using anti-PER2 antibody. The SCN of these mice were collected in the morning when the endogenous PER2 protein is normally at its nadir. As expected, after 7 days, high levels of PER2 expression was detected in the water-maintained *Nms-Per2* mice while the Dox-administered mice exhibit minimal PER2 immunoreactivity that is comparable to the *R26-Per2* control mice (Figure 2-2). Therefore, the *Per2* transgene can be reversibly overexpressed in *Nms-Per2* mice.

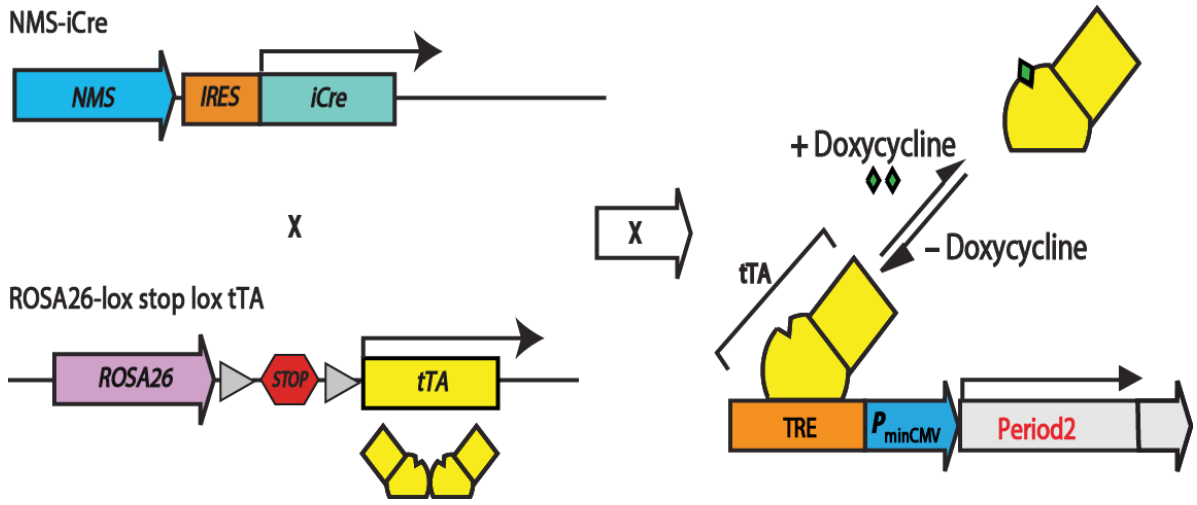

Figure 2-1. Schematic diagram showing the Tet-Off system and constructs used for generating the *Nms-Per2* mice. The *Nms* promoter drive the expression of iCre, which excises the stop codon flanked by loxP, thereby allowing ROSA26 to express tTA. tTA binds to the tetO promoter in the absence of doxycycline (Dox) but not in its presence, resulting in transcriptional activation or repression of the *Per2* transgene, respectively.

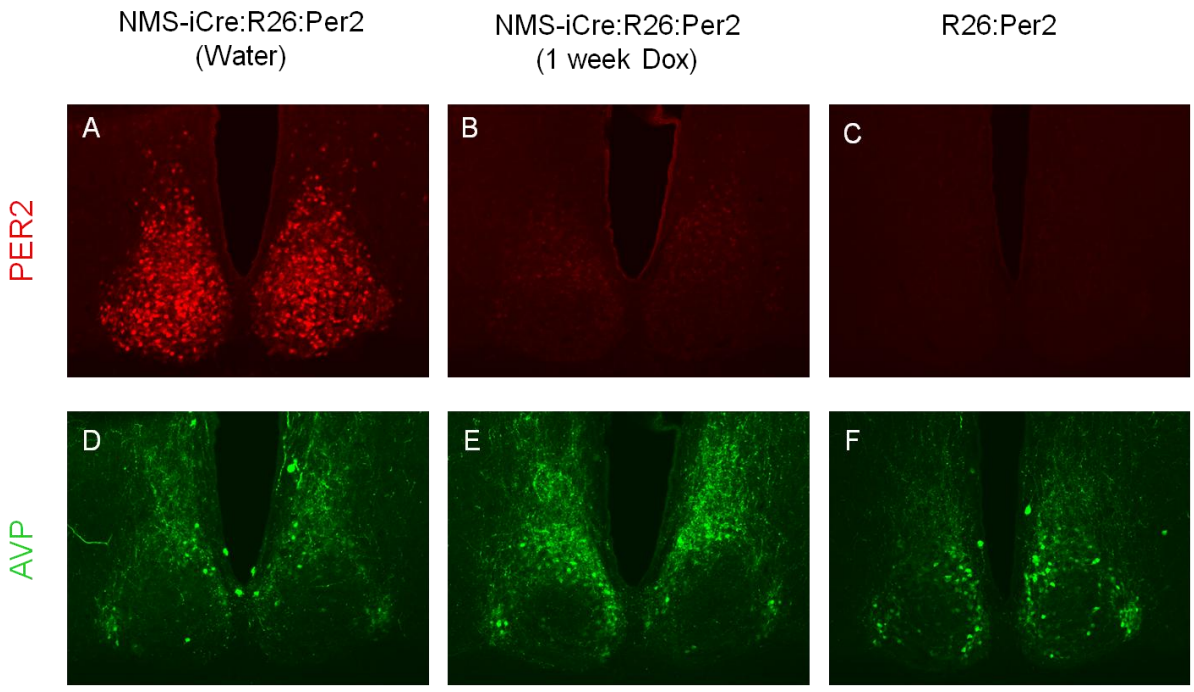

Figure 2-2. The *Per2* transgene can be reversibly overexpressed in *Nms*-positive neurons of the SCN. Representative images captured with a 10X objective are displayed. The SCN of water-administered *Nms-Per2* (A and D), Dox-administered *Nms-Per2* SCN (B and E), and water-administered *R26-Per2* mice (C and E) were stained with anti-PER2 and anti-AVP in the morning when endogenous PER2 protein expression is low. One week of Dox nearly turned off all *Per2* transgene expression in *Nms-Per2* mice.

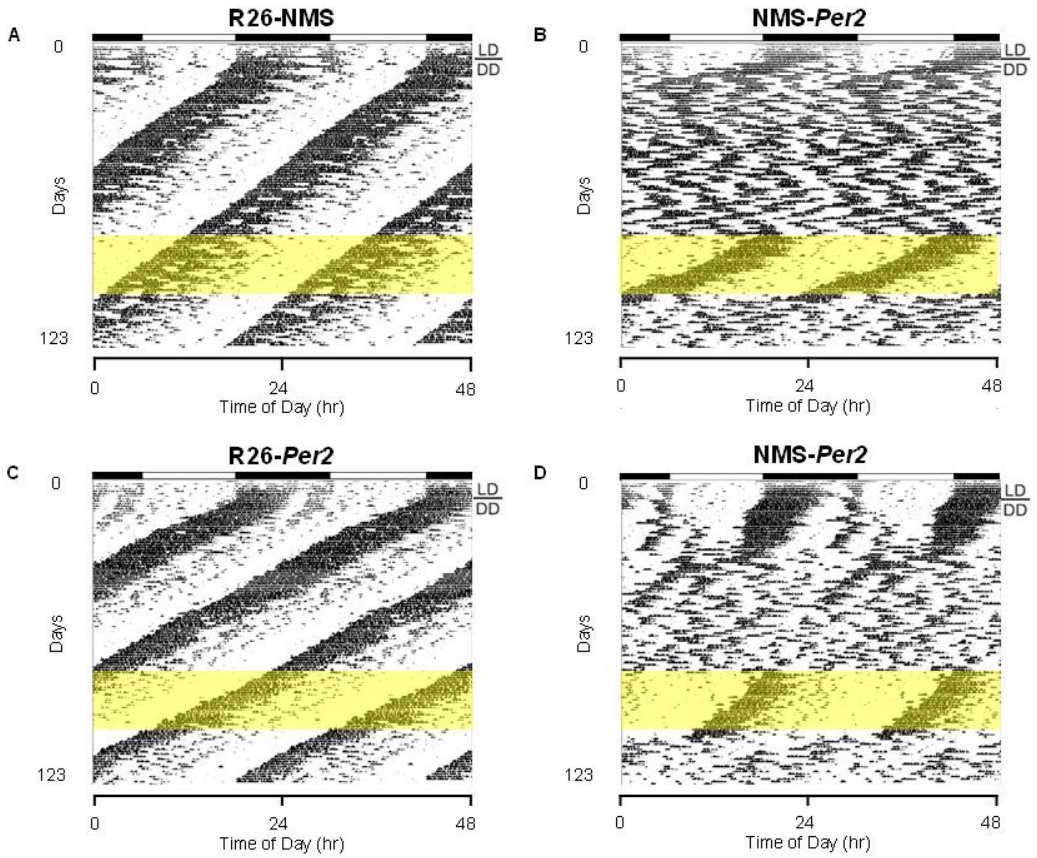

Figure 2-3. Locomotor activity records of *Nms-Per2* transgenic and littermate controls. Representative actograms of A) *R26-Nms*; C) *R26-Per2*; B) and D) *Nms-Per2* mice. *Nms-Per2* mice displayed a loss of rhythmicity after a prolonged time in DD compared to controls. Normal circadian rhythms are restored in *Nms-TeNT* upon Dox administration (highlighted in yellow). Control mice exhibit no significant changes in free-running period before and after Dox.

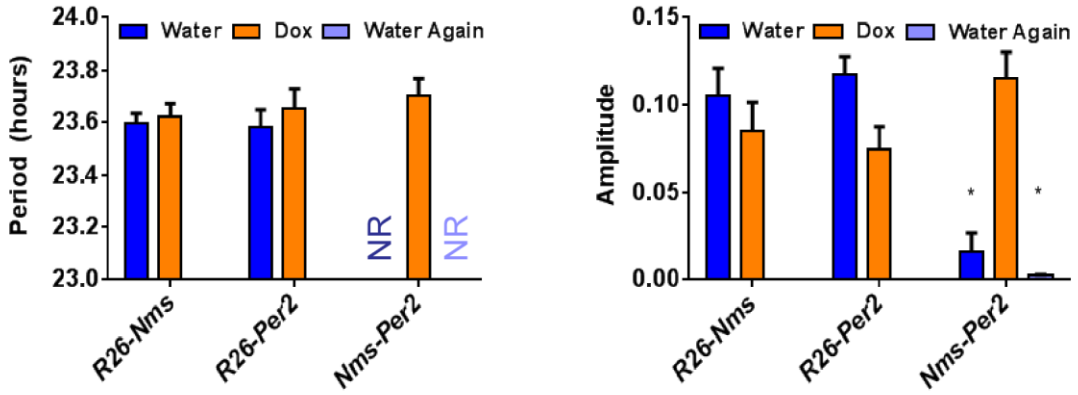

Figure 2-4. Quantification of circadian activity in *Nms-Per2* transgenic and littermate controls. Average free-running periods as well as FFT power (amplitude) were calculated for all mice during water and Dox treatments. Values are presented as mean ± SEM. The loss of circadian rhythms in water-treated *Nms-Per2* mice is indicated by the low average FFT power in the circadian spectrum. These values are returned to levels not significantly different from controls by Dox treatment. *R26-Nms*, n=13; *R26-Per2*, n=11; *Nms-Per2*, n=15; $p<0.5$ by Two-Way ANOVA.

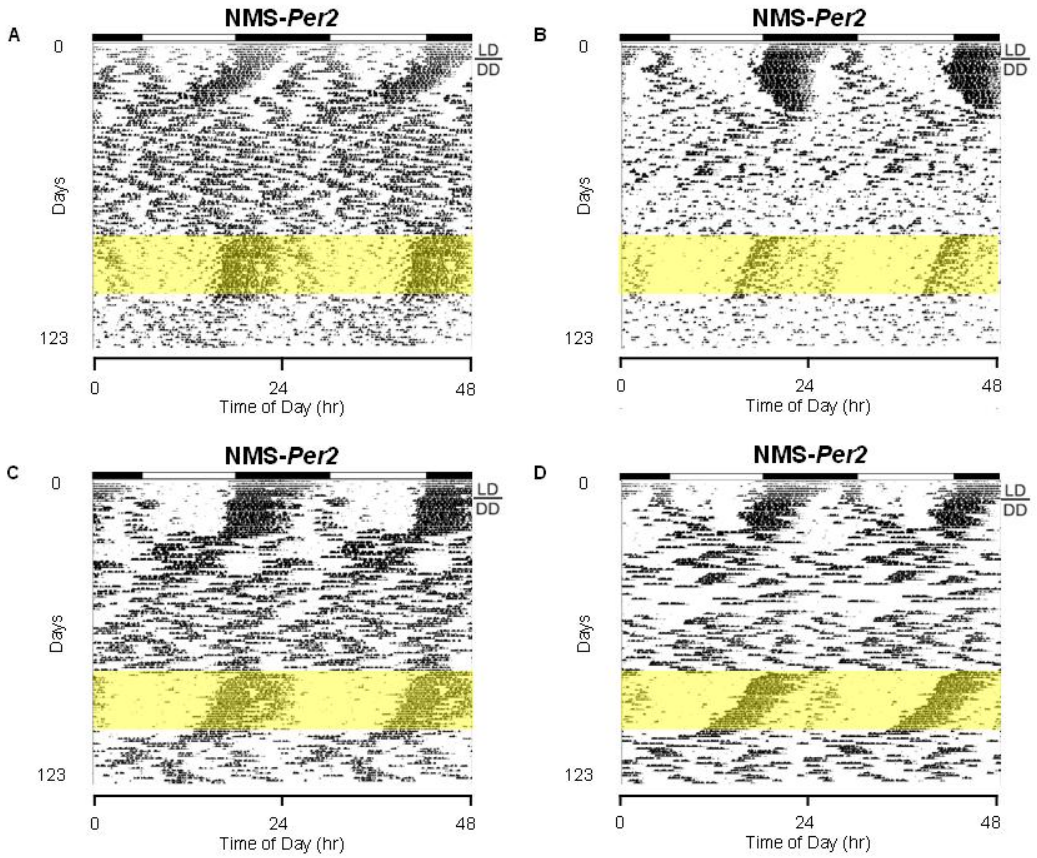

Figure 2-5. More representative locomotor activity records of *Nms-Per2* transgenic mice. Times of Dox administration are highlighted in yellow.

***Nms-Per2* mice gradually loses circadian rhythms in behavior**

Locomoter wheel running activity was utilized to assess the behavioral circadian rhythms of *Nms-Per2* mice. *Nms-Per2* mice contain two copies of ROSA26-lox-stop-lox-tTA along with a single copy of *Nms-iCre* and *tetO-Per2*, while the control mice also contain the homozygous ROSA26-lox-stop-lox-tTA loci but lack either *tetO-Per2* or *Nms-iCre* (referred to as *R26-Nms* and *R26-Per2*, respectively). Under 12:12 LD cycle, all mice exhibit normal bouts of restricted nighttime activity during the dark phase. Upon release into constant darkness (DD), *Nms-Per2* initially exhibited normal running rhythms as do the control mice (Figures 2-3, 2-4, and 2-5). After a prolonged period of time in DD, however, *Nms-Per2* mice displayed an apparent loss of circadian rhythms while the controls maintain robust running rhythms. Variability was observed in the amount of time it takes for an individual *Nms-Per2* mouse to lose its circadian rhythms, but 15 out of 15 mice exhibit disruptions of behavioral daily rhythms. To examine whether the loss of circadian rhythms can be recovered when the *Per2* transgene is turned off, 10 μg/ml of doxycycline (Dox) was administered in drinking water. Upon Dox administration, control mice continued to run with unaltered rhythms, while *Nms-Per2* mice displayed a rapid recovery of circadian period with a mean period comparable to that of the controls (Figures 2-3, 2-4, and 2-5). Re-administration of water to turn on the *Per2* transgene once again causes *Nms-Per2* mice to lose circadian rhythmicity (Figures 2-3, 2-4, and 2-5). These results indicate that the disruption of circadian rhythms is dependent on the overexpression of the *Per2* transgene. Thus, the conditional overexpression of *Per2* in *Nms*-producing cells is sufficient to disrupt the behavioral circadian rhythms of mice.

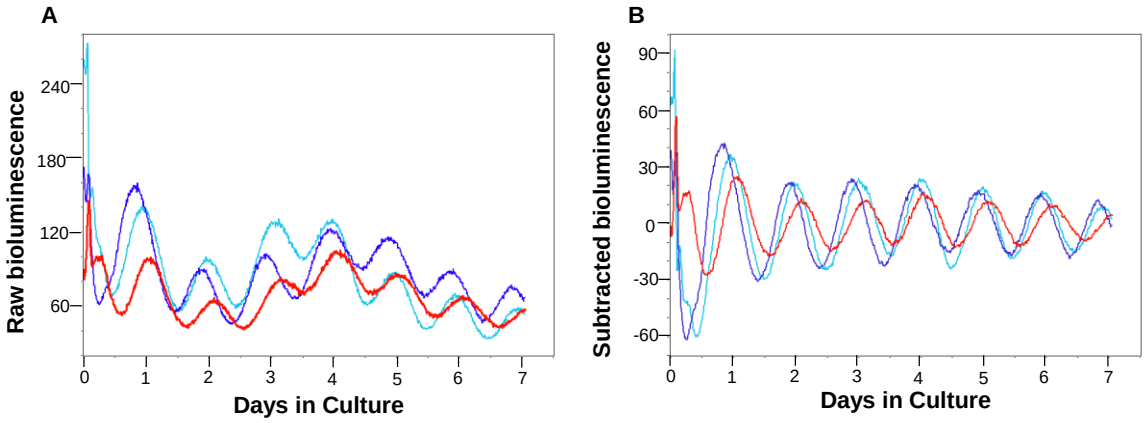

Figure 2-6. Representative bioluminescence records showing PER2::LUC rhythms from the SCN of *Nms-Per2* mice and littermate controls. Raw (A) and baseline-subtracted (B) plots of the SCN of *R26-Nms* (light blue trace), *R26-Per2* (dark blue trace), and *Nms-Per2* (red trace) are shown. The SCN of *Nms-Per2* mice display lower amplitudes compared to the SCN of littermate controls.

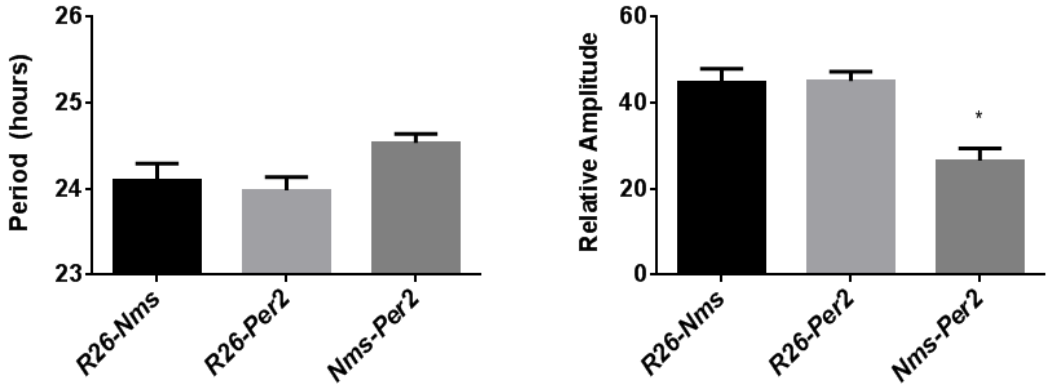

Figure 2-7. Quantification of PER2::LUC Amplitude in *Nms-Per2* transgenic and littermate controls. Values are presented as mean ± SEM. The SCN of *Nms-Per2* mice exhibited lower amplitudes of PER2::LUC rhythms compared to controls ($p < 0.05$ for each comparison). No significant differences in mean circadian period were found in controls. *R26-Per2*, n=5; *R26-Nms*, n=11; *Nms-Per2*, n=6.

Nms-Per2 SCN display lower amplitude of PER2::LUC rhythms

To examine the cellular and molecular effects of *Per2* overexpression in *Nms*-producing cells of the SCN, we crossed *Nms-Per2* mice with mice carrying the PER2::LUC reporter (Yoo et al., 2004). SCN organotypic cultures from *Nms-Per2* mice displayed lower amplitudes on average with a period that is slightly longer but not significantly different from controls (Figures 2-6 and 2-7). The finding of rhythmic oscillations of PER2::LUC is somewhat surprising but not totally unexpected because molecular rhythms of non-*Nms* cells may still persist, perhaps less synchronously, leading to the appearance of low amplitude PER2::LUC rhythms on the SCN tissue level.

Loss of _Nms_ signaling does not abolish behavioral circadian rhythms

Having identified *Nms* neurons as a population of cells that are necessary and sufficient for the generation of behavioral circadian rhythms, we sought to elucidate the intercellular mechanisms by which *Nms* pacemaking cells communicate with other cells to coordinate synchrony of the SCN cellular network. Since neuropeptides have been implicated to play an important role in neuronal coupling, we evaluated the role of the NMS peptide in regulating behavioral circadian rhythms. We generated knockout mice lacking the *Nms* gene ($Nms^{-/-}$) by targeted deletion of its signal peptide sequence. After verifying that no NMS peptide is detected in the SCN of $Nms^{-/-}$ mice (Figure 3-1), we also generated mutant mice that lack both *Nms* and its closely related paralog, *neuromedin U* (*Nmu*) by breeding $Nms^{-/-}$ with $Nmu^{-/-}$ mice (Hanada et al., 2004). To determine the impact of the loss of *Nms/Nmu* signaling on *in vivo* rhythms, we monitored wheel-running activity in LD and in

DD. *Nms*$^{-/-}$, *Nmu*$^{-/-}$, and *Nms*$^{-/-}$*Nmu*$^{-/-}$ mice all exhibited normal entrainment to light and free-running activity rhythms no different from wild-type (WT) littermates (Figure 3-1), suggesting that *Nms/Nmu* signaling is not required for the generation of behavioral circadian rhythms.

TeNT transgenic overexpression is inducible and reversible in *Nms-TeNT* mice

Observations made by several groups have suggested that a considerable amount of redundancy is present to generate and maintain circadian rhythmicity. *In vitro*, neuropeptides such as VIP, AVP, and GRP are all likely capable of acting as synchronizing agents (Brown et al., 2005; Maywood et al., 2006a, 2011). *In vivo*, a percentage of mice lacking *Vip* or *Vipr2* lose circadian rhythmicity (Aton et al., 2005; Colwell et al., 2003; Hughes et al., 2004, 2008), suggesting that although VIP is likely a prominent intercellular mediator, additional signaling pathways exist to compensate for its loss. Likewise, the disruption of other synaptic cues such as AVP, GRP, prokineticin 2 (PK2), histamine, and cholecystokinin (CCK) leads to behavioral phenotypes ranging from apparently normal to some degree of disruption with incomplete penetrance (Table S1) (Abe et al., 2004; Aida et al., 2002; Li et al., 2009; Mistlberger et al., 2001). These published findings and our observations of normal behavioral rhythms in *Nms*$^{-/-}$*Nmu*$^{-/-}$ mice prompted us to ask whether inhibiting the release of all synaptic mediators in *Nms* cells will abolish circadian rhythmicity or can other forms of signaling mechanisms such as gap junctions and gasotransmitters compensate. To address this question, we crossed *Nms-iCre* and ROSA26-lox-stop-lox-tTA mice with transgenic mice that express a fusion gene of tetanus toxin light chain (TeNT) and enhanced green

fluorescent protein (EGFP) under the tetracycline-responsive promoter (Hikida et al., 2010; Yamamoto et al., 2003). The resulting mouse line (*Nms-TeNT*; Figure 3-2) contains two copies of ROSA26-lox-stop-lox-tTA and a single copy of *Nms-iCre* and TeNT. TeNT is an endopeptidase specific for VAMP2, which is required for activity-dependent synaptic release of neurotransmitters (Schoch et al., 2001). To determine that the TeNT transgene can be overexpressed in a reversible manner, water-maintained and Dox-administered *Nms-TeNT* mice, along with control mice lacking *Nms-iCre* (*R26-TeNT*) were immunostained with anti-GFP. As expected, GFP was expressed robustly and restrictively in the SCN (Figure 3-3) with minimal to no signals detected outside of the SCN (data not shown). After 7 days of Dox administration, GFP expression was almost completely repressed (Figure 3-3). The *R26-TeNT* control mouse line exhibits no GFP immunoreactivity, indicating the lack of TeNT expression leakage. Therefore, the TeNT transgene can be conditionally overexpressed in *Nms-TeNT* mice.

Nms-TeNT mice gradually loses circadian rhythms in behavior

Locomoter wheel running activity was utilized to assess the behavioral circadian rhythms of *Nms-TeNT* mice. The littermate controls include mice that lack either the TeNT transgene (referred to as *R26-Nms*), the *Nms-iCre* (referred to as *R26-TeNT*), or contain only ROSA26-lox-stop-lox- tTA (referred to as *R26*). All mice were raised on 20 μg/ml of Dox to exclude effects of TeNT expression during development. Mice of adult age were placed on wheels in a 12:12 LD cycle for at least 7 days while administered with Dox. After at least >2 weeks of DD, Dox was replaced with water and the mice continued to free-run until a clear

phenotype is observed. Dox was once again re-administered to demonstrate reversibility of the phenotype. As seen in Figures 3-4 and 3-5, under Dox administration, *Nms-TeNT* exhibit a circadian period comparable with the control mice. Upon switching to water, all *Nms-TeNT* mice gradually lose their behavioral circadian rhythms. Re-administration of Dox gradually rescues the disrupted daily rhythms. Curiously, 3-6 weeks of time were needed for *Nms-TeNT* mice to both lose and recover behavioral rhythmicity.

Nms-TeNT SCN has a lower amplitude of PER2::LUC rhythms

To examine the cellular and molecular effects of TeNT overexpression in *Nms*-producing cells of the SCN, we crossed *Nms-TeNT* mice with mice carrying ROSA26-lox-stop-lox-tTA and PER2::LUC (see Methods). SCN organotypic cultures from *Nms-TeNT* mice displayed lower amplitudes on average with a period within the normal range (Figures 3-7 and 3-8). Much like the *Nms-Per2* mice, the finding of rhythmic oscillations of PER2::LUC is somewhat surprising but not totally unexpected because neurotransmission of non-NMS cells are still intact and may allow for the persistence of less synchronous molecular rhythms that can lead to the appearance of PER2::LUC rhythms on the SCN tissue level. These remaining rhythms apparently, are not sufficient to generate circadian rhythms on the behavioral level.

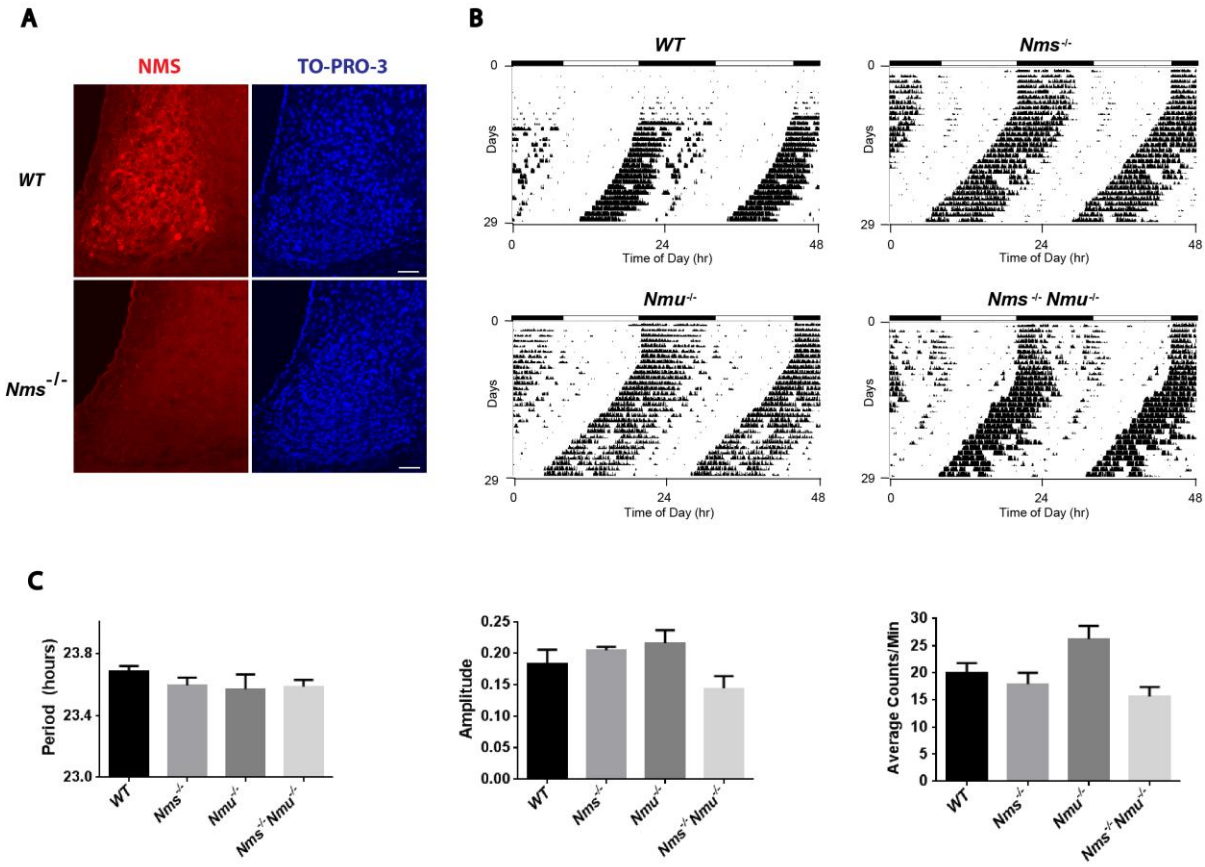

Figure 3-1. *Nms*$^{-/-}$ *Nmu*$^{-/-}$ mice exhibit normal free-running circadian activity.
(A) Immunostaining of NMS peptide (red) on SCN sections of colchicine-treated *Nms knockout mice* (*Nms*$^{-/-}$) and C57B/6J wild-type (WT) mice. TO-PRO-3 counterstains the nuclei. NMS immunoreactivity was not detected in *Nms*$^{-/-}$ mice.
(B) Representative actograms of C57B/6J WT (top-left panel), *Nms*$^{-/-}$ (top-right panel), *neuromedin u knockout* (*Nmu*$^{-/-}$) (bottom-left panel), and *neuromedin s/neuromedin u double knockout* (*Nms*$^{-/-}$/*Nmu*$^{-/-}$) mice (bottom-right panel).
(C) Quantification of circadian activity in C57B/6J WT, *Nms*$^{-/-}$, *Nmu*$^{-/-}$, and *Nms*$^{-/-}$/*Nmu*$^{-/-}$ mice. Mean free-running period/amplitude and activity counts were not significantly different between genotypes ($p>0.05$; WT, n=5; *Nms*$^{-/-}$, n=8; *Nmu*$^{-/-}$, n=5; *Nms*$^{-/-}$/*Nmu*$^{-/-}$, n=15). Values are presented as mean ± SEM.

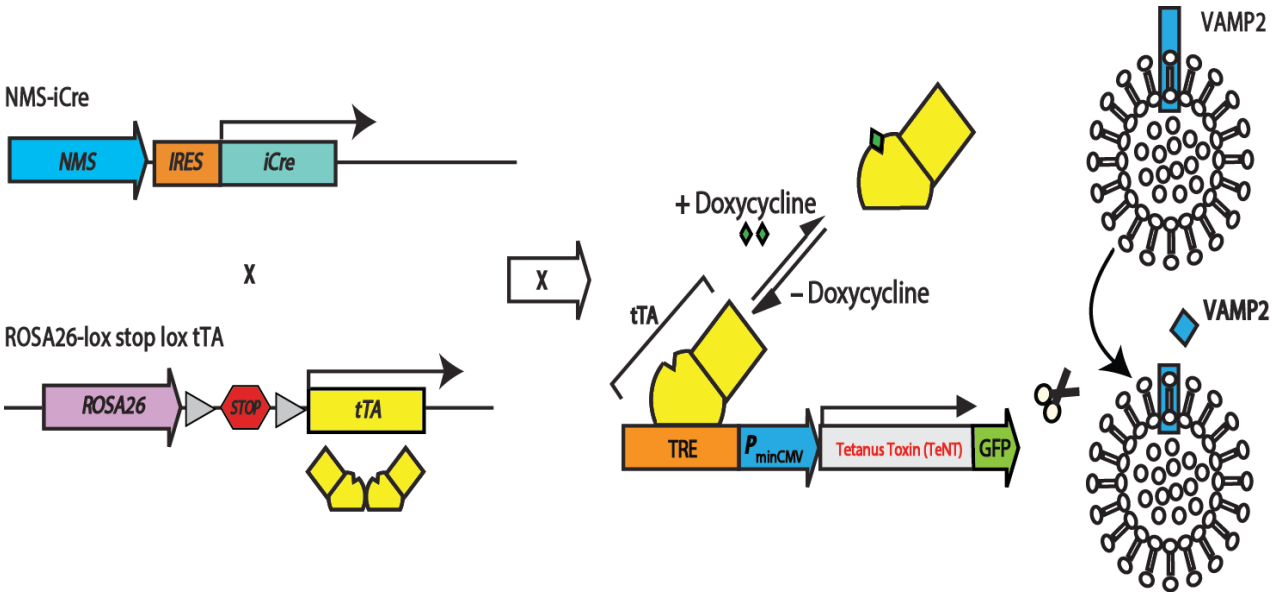

Figure 3-2. Schematic diagram showing the Tet-off system and constructs used for generating the *Nms-TeNT* mice. The *Nms* promoter drive the expression of iCre, which excises the stop codon flanked by loxP, thereby allowing *Rosa26* to overexpress tTA. tTA binds to the *tetO* promoter in the absence of doxycycline (Dox) but not in its presence, resulting in transcriptional activation or repression of the downstream transgene (*TeNT*), respectively.

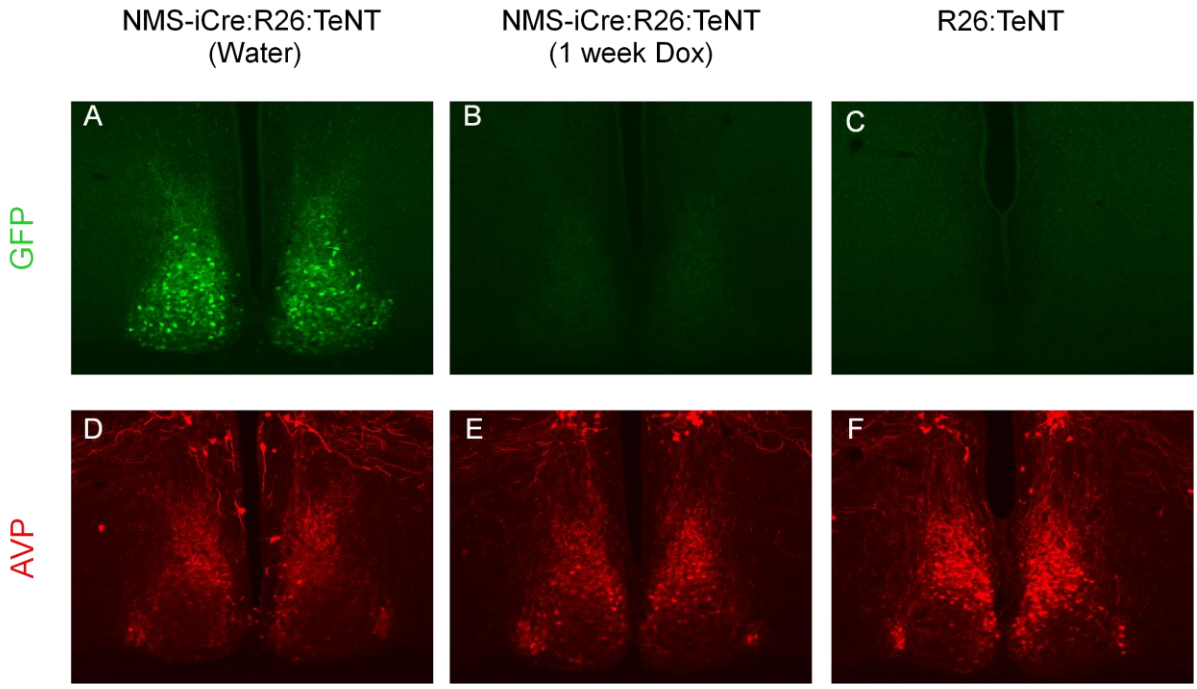

Figure 3-3. The TeNT transgene can be reversibly expressed in *Nms*-expressing neurons of the SCN. Representative images captured with a 10X objective are shown. The SCN of water-administered *Nms-TeNT* (A and D), Dox-administered *Nms-TeNT* SCN (B and E), and water-administered *R26-TeNT* mice (C and E) were stained with anti-GFP and anti-AVP. One week of Dox nearly turned off all TeNT transgene expression in *Nms-TeNT* mice.

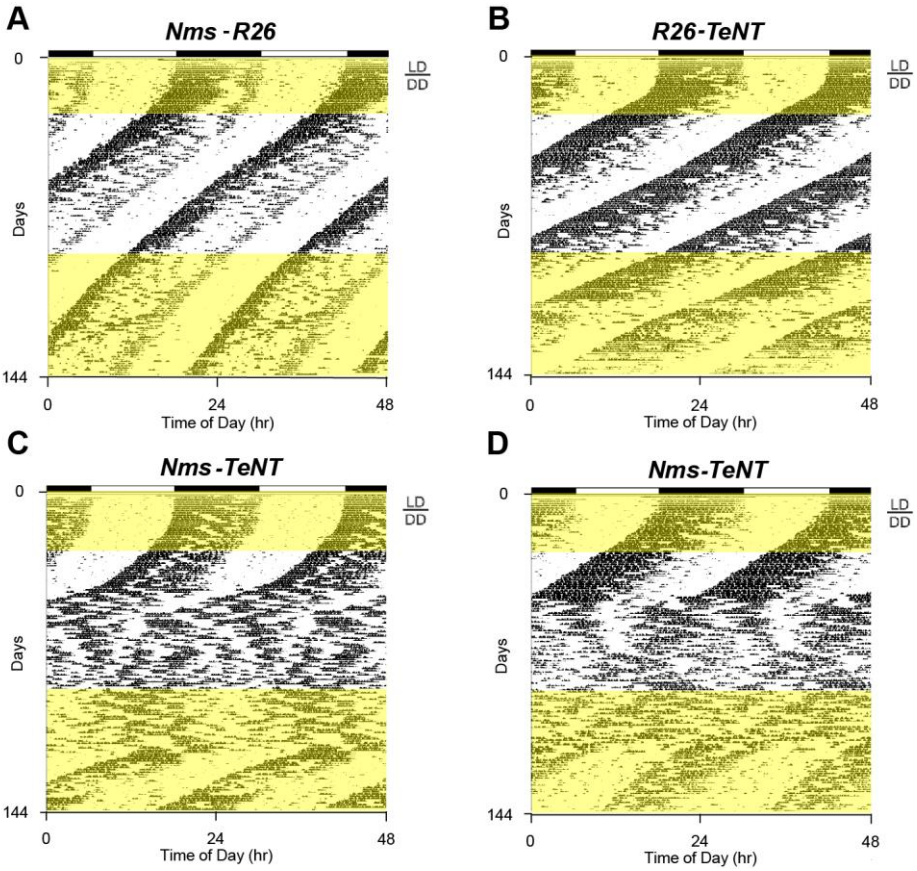

Figure 3-4. Locomotor activity records of *Nms-TeNT* transgenic and littermate controls. Representative actograms of A) *R26-TeNT*; B) *R26-Nms*; C) and D) *Nms-TeNT* mice. *Nms-TeNT* and littermate controls were raised and maintained on Dox (highlighted in yellow) in LD and for >2 weeks in DD. Upon switching to water, *Nms-TeNT* exhibited a loss of rhythmicity after a period of normal free-running. Re-administration of Dox restores the mice to normal behavioral rhythms. Control mice displayed an unaltered normal free-running period before and after Dox.

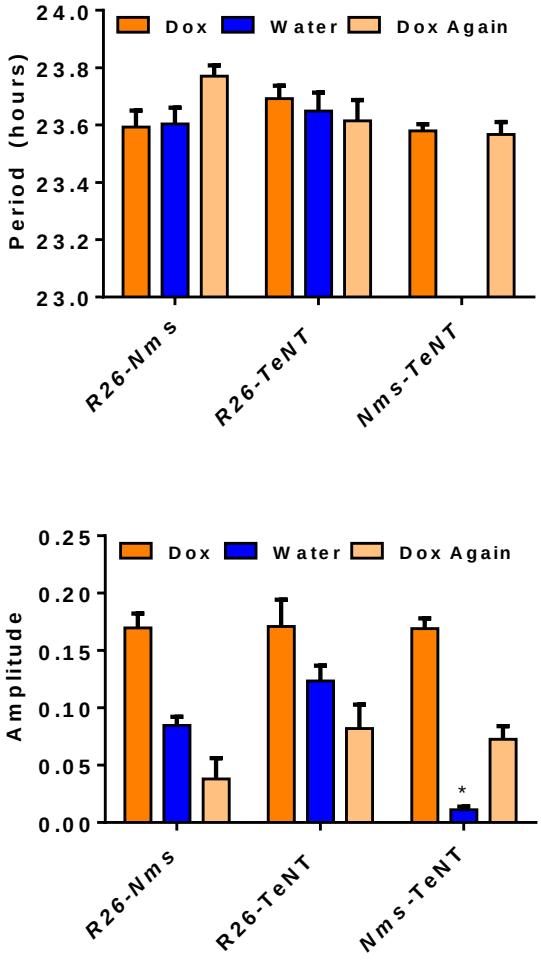

Figure 3-5. Quantification of circadian activity in *Nms-TeNT* transgenic and littermate controls. Average free-running periods as well as FFT power (amplitude) were calculated for all mice. All values (mean ± SEM) are calculated using the 21 days prior to the change in Dox or water treatment. The normal free-running period after the re-administration of Dox are not quantified here. The loss of circadian rhythms in water-treated *Nms-TeNT* mice is indicated by NR in period values and the low average FFT power in the circadian spectrum. These values are returned to levels not significantly different from controls by Dox treatment. *R26-Nms*, n=8; *R26-TeNT*, n=10; *Nms-TeNT*, n=29.

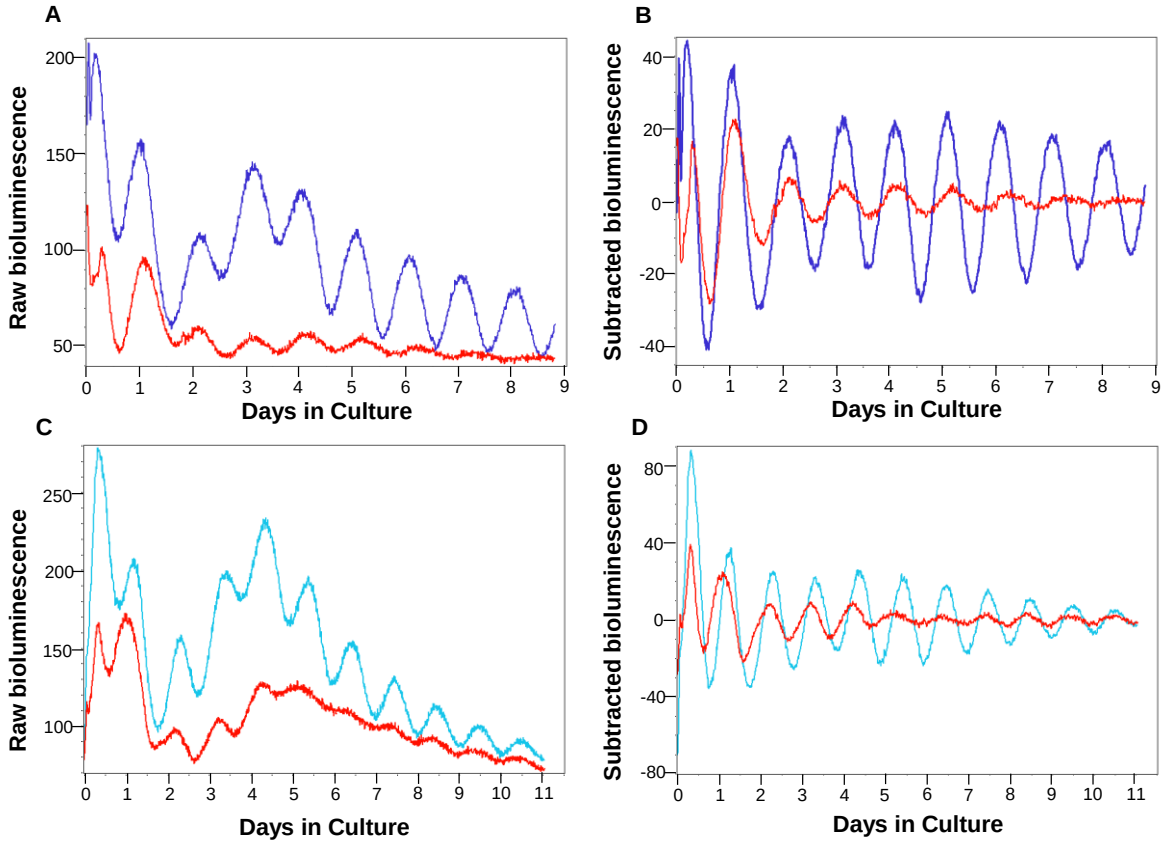

Figure 3-6. Representative bioluminescence records showing PER2::LUC rhythms from the SCN of *Nms-TeNT* mice and littermate controls. Raw (A and C) and baseline-subtracted (B and D) plots of the SCN of *R26-Nms* (light blue trace), *R26-TeNT* (dark blue trace), and *Nms-TeNT* (red trace) are shown. The SCN of *Nms-TeNT* mice display lower amplitudes compared to the SCN of littermate controls.

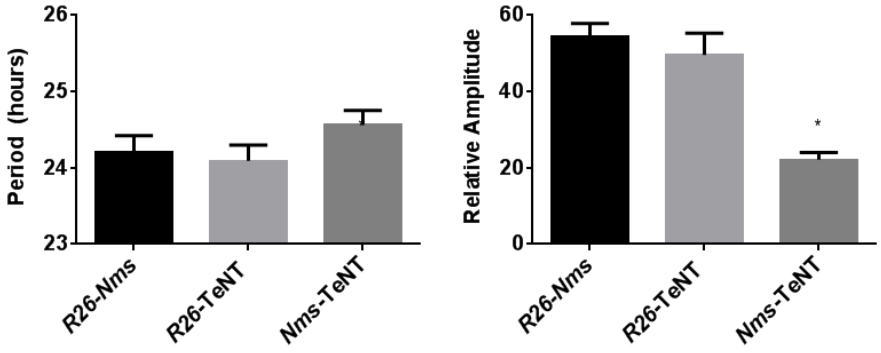

Figure 3-7. Quantification of PER2::LUC amplitude in *Nms-TeNT* transgenic and littermate controls. Values are presented as mean ± SEM. The SCN of *Nms-TeNT* mice exhibited lower amplitudes of PER2::LUC rhythms compared to controls ($p < 0.05$ for each comparison). No significant differences in mean circadian period were found in controls. *R26*, n=8; *R26-TeNT*, n=7; *R26-Nms*, n=7; *Nms-TeNT*, n=8.

CHAPTER FOUR
General Discussion

In an effort to better understand the cellular basis of circadian rhythms, we utilized three complementary approaches to ask whether a subset of SCN neurons marked by NMS is sufficient and required for the generation of circadian rhythms. Using the *Nms-Clock*$^{\Delta 19}$ mice, we found that lengthening the molecular rhythms of NMS-producing cells was sufficient to lengthen the circadian period on a behavioral level. Likewise, in the *Nms-Per2* mice, we observed that abolishing the intracellular rhythms of NMS-producing neurons by overexpressing *Per2* sufficiently lead to the complete loss of behavioral circadian rhythms. Taken together, these two approaches demonstrate that behavioral circadian rhythms can be controlled by NMS-producing cells of the SCN. The capability of NMS-expressing neurons to exert control over behavior, however, does not imply that these cells are required for the generation of behavioral circadian rhythms. Therefore, to determine whether NMS-positive cells of the SCN are required for producing circadian rhythms on a behavioral level, we produced *Nms-TeNT* mice and observed that when neurotransmission is disrupted in NMS-producing neurons, behavioral circadian rhythm is lost. Altogether, our results suggest that NMS-expressing neurons are sufficient and essential to generate daily rhythms in behavior.

Characterization of *Nms-Clock*$^{\Delta 19}$ mice

The *Clock*$^{\Delta 19}$ mutation was initially identified as a dominant negative mutation resulting from an A→T nucleotide transversion that causes the deletion of exon 19 and the

truncation of 51 amino acids in the C-terminus (Vitaterna et al., 1994). *Clock*$^{\Delta 19}$ heterozygous mice have a circadian period of 24.4 h, approximately 1 hour longer than the period of wild-type mice. Precedence for using the *Clock*$^{\Delta 19}$ mice as a tool to elucidate behavioral circadian rhythms can be first found in a study utilizing *Clock*$^{\Delta 19}$ mouse aggregation chimeras (Low-Zeddies and Takahashi, 2001, 2005). In this study, populations of chimeras that cover a wide range of proportions of wild-type versus *Clock*$^{\Delta 19}$ homozygous or heterozygous mutant cells were created to assess how cells of contrasting genotype functionally interact in the SCN to control circadian behavior. The findings of this study indicate that, with a few exceptions, the proportion of the number of *Clock*$^{\Delta 19}$ mutant cells correlates positively with the severity of the phenotype. Subsequently, in an effort to better understand spatial and temporal control of the *Clock*$^{\Delta 19}$ mutation in the brain, transgenic mice that express *Clock*$^{\Delta 19}$ under the transcriptional regulation of the *Scg2* promoter were generated (Hong et al., 2007). These mice, which have a lengthened period of ~24.5 h, were found to express *Clock*$^{\Delta 19}$ in >90% of the SCN cells. In contrast to the chimeric *Clock*$^{\Delta 19}$ mice, though, all cells of the *Scg2* promoter-driven *Clock*$^{\Delta 19}$ transgenic mice contain two wild-type copies of *Clock*. In the study presented in this dissertation, we found that *Clock*$^{\Delta 19}$ mutant expression only in ~40% of SCN marked by NMS lead to a lengthened behavioral circadian period of ~24.6 hours, comparable to the period length of double transgenic mice expressing *Clock*$^{\Delta 19}$ under the regulation of *Scg2*. Questions now remain whether the ability of NMS-producing cells to control the behavioral phenotype is due to its absolute number of expression or due to its unique localization within the SCN. In other words, will expressing the *Clock*$^{\Delta 19}$ mutant gene in any ~40% of the SCN cells lead to a lengthened period in

behavioral rhythms? Alternatively, will *Clock*$^{\Delta 19}$ mutant expression in a smaller number of cells located in SCN regions marked by NMS cause a longer period length? In other words, are there subpopulations of NMS-expressing cells that play a critical role in generating coherent rhythms? The former question related to the percentage of NMS expression is difficult to answer due to the lack of other Cre drivers with expression in exactly ~40% of the SCN cells. Conceivably, one can perform chimeric aggregation studies using wild-type cells with cells that express *Clock*$^{\Delta 19}$ along with two normal copies of *Clock*. Alternatively, AAV expression of *Clock*$^{\Delta 19}$ in ~40% of the SCN cells can also be performed to address the question. The second question related to the significance of the regional distribution of NMS, can be addressed in part by using transgenic lines that express Cre under the promoter of VIP or AVP. Since, NMS is expressed in the majority of VIP- and AVP-expressing neurons, it is possible that the lengthening of behavioral rhythms in *Nms-Clock*$^{\Delta 19}$ mice may be due to *Clock*$^{\Delta 19}$ expression in either or both VIP- or AVP- cells. Using a VIP-Cre or AVP-Cre in place of *Nms-iCre* in our combinatorial genetic approach will resolve this question.

Characterization of *Nms-Per2* mice

Period2 (Per2) is an essential core clock gene involved in the negative limb of the molecular feedback loop. Constitutive overexpression of *Per2* in the liver or fibroblast have been demonstrated to ablate the molecular circadian rhythms of the tissue or cell, respectively (Chen et al., 2009b). Abolishing the oscillation of *Per2* in the SCN using double transgenics expressing *Scg2*-promoter driven tTA and *tetO-Per2* (*Scg2-Per2*) has also been shown to lead to the lack of behavioral circadian rhythms (Chen et al., 2009b). In this

dissertation, we show that the constitutive overexpression of *Per2* in only NMS-producing cells of the SCN causes the loss of behavioral rhythms. This phenotype is similar to the transgenic mice expressing *Per2* under the *Scg2* promoter with one key difference. *Scg2-Per2* mice immediately lose behavioral circadian rhythms upon release into constant darkness. In contrast, once released into darkness from 12:12 LD cycle, *Nms-Per2* mice initially free-runs normally, and then exhibit a loss of daily rhythms after a prolonged period of time in constant darkness. This notable difference suggests that light entrainment seems to have prolonged and significant effects on the behavior of *Nms-Per2* mice. *Per2* has been implicated to play a role in the light resetting response of the SCN because it is rapidly induced by light (Albrecht et al., 1997; Shearman et al., 1997; Shigeyoshi et al., 1997; Zylka et al., 1998) . It has been suggested that light resetting occurs through the binding of phosphorylated CREB onto the CRE elements of the *Per* promoters (Travnickova-Bendova et al., 2002). Therefore, one possible explanation for the prolonged period of time needed for *Nms-Per2* mice to lose circadian rhythms in behavior is that *Nms*-producing cells contain retinorecipient neurons that receive light-induced signal transduction through the retinohypothalamic tract. Initially, the effect of light may be able to reset the oscillation of *Per2*, but after a prolonged period of time without light cues, *Per2* oscillation is abolished by constitutive overexpression and behavioral rhythms are lost. Since *Scg2* is also expressed in the retina of the eye (Overdick et al., 1996; Troger et al., 2005), which maintains robust circadian oscillations (Tosini et al., 2007), it is more difficult to interpret the lack of delay in the loss of daily rhythms in *Scg2-Per2* mice.

Characterization of *Nms-TeNT* mice

In recent years, tetanus toxin has been used extensively to determine the function of particular cell populations by assessing the consequences of inhibiting their neurocircuitry (Hikida et al., 2010; Kim et al., 2009; Nakashiba et al., 2008, 2009, 2012; Suh et al., 2011; Yamamoto et al., 2003). In contrast to diphtheria toxin, one major advantage of using this toxin is that cell toxicity is not observed and the inhibition of neurotransmission is fully reversible. Therefore, reorganization of cellular network due to cell death is minimized. In this dissertation, we report that the expression of TeNT in *Nms*-producing neurons of the SCN causes the loss of behavioral circadian rhythms. This strongly suggests that synaptic neurotransmission of *Nms*-expressing cells are normally required to generate coherent behavioral rhythms. Although we cannot rule out that the inhibition of neurotransmission in other SCN neurons may also lead to similar disruptions of daily rhythms, the remaining functional neurons were unable to compensate for the loss of synaptic neurotransmission from *Nms*-producing neurons in *Nms-TeNT* mice. Curiously, it takes several weeks for *Nms-TeNT* mice to lose circadian rhythmicity when TeNT is induced and several weeks for the mice to regain circadian rhythms upon Dox administration. This is likely due to the chain of molecular events that must occur for synaptic neurotransmission to be inhibited. The induction of the TeNT by Dox withdrawal is estimated to be within days (unpublished data) while the suppression of TeNT, which has a half-life around ~5-6 days in culture (Habig et al., 1986) occurs within one week in our genetic model (Figure 3-2). Following TeNT expression or suppression, VAMP2, the molecular target of TeNT, needs to become cleaved or re-synthesized for behavioral rhythms to be lost or recovered, respectively. The *in vitro*

synthesis rate of VAMP2, is about one week, as is its half-life (Daly and Ziff, 1997). Downstream of VAMP2, the synthesis/release of neurotransmitters or the degradation of neurotransmitters must occur for activity-dependent neurotransmission to recover or to stop, respectively. These processes may contribute to the prolonged period of time needed for *Nms-TeNT* mice to lose or recover rhythms. Alternatively, the process of synchronization or desynchronization between SCN neurons may take an extended amount of time under conditions without light entrainment. Our study is the first to examine the *in vivo* dynamics of synchronization and desynchronization of SCN neurons under no influence from environmental light. As with *Nms-Per2* mice, *Nms-TeNT* mice lose circadian rhythm in constant darkness but are able to entrain to 12:12 LD cycle. This also raises the possibility that *Nms*-positive cells contain light-responsive neurons that are able to receive light-induced signals presynaptically even while postsynaptic outputs of *Nms*-expressing neurons are blocked.

Coupling versus output

Using three complementary approaches, we demonstrated that NMSergic neurons are capable of controlling the behavioral output in circadian rhythms. This regulation can occur by direct output from *Nms*-producing neurons to efferent pathways of the SCN or first by synchronization with non- *Nms*-producing cells. To address these two non-mutually exclusive possibilities, we assessed the PER2::LUC rhythms of all three groups of mice to observe the molecular rhythms of the SCN as a whole. Since *Nms*-producing cells represent ~40% of all SCN neurons, if non-*Nms* neurons continue to oscillate with a normal period (i.e.

no cellular coupling is present), then one would expect the period of the PER2::LUC rhythms of the SCN as a whole to be close to that of the wild-type SCN. In contrast, we found the PER2::LUC rhythms of *Nms-Clock*$^{\Delta 19}$ SCN to oscillate robustly with a longer period compared to that of the control SCN, suggesting that cellular coupling between NMS and non-NMS cells are present to synchronize the molecular rhythms of two cell populations. Since VIP-positive neurons also express NMS, our findings are consistent with the reports that VIP-deficient SCN exhibit significant losses in their ability to synchronize daily rhythms (Ciarleglio et al., 2009; Maywood et al., 2006b, 2011). The PER2::LUC rhythms of the *Nms-Per2* and *Nms-TeNT* SCN, interestingly, both exhibit oscillations with lower amplitudes. Given that *Nms*-producing cells are likely involved in the synchronization of SCN neurons, as evident from the lengthened period in the SCN of *Nms-Clock*$^{\Delta 19}$ mice and reports that VIP is a critical intercellular synchronizing mediator, the reduced amplitudes observed in *Nms-Per2* and *Nms-TeNT* mice can be best explained by reduced synchrony amongst SCN cells due to the loss of rhythms or synaptic signaling in *Nms*-producing cells. Alternatively, lower amplitudes of PER2 oscillation across all individual SCN cells can also lead to reduced amplitude of oscillations on a tissue level. To rule out this possibility, single-cell bioluminescent recording will need to be performed in the future.

BIBLIOGRAPHY

Abe, H., Honma, S., Ohtsu, H., and Honma, K.-I. (2004). Circadian rhythms in behavior and clock gene expressions in the brain of mice lacking histidine decarboxylase. Brain Research. Molecular Brain Research *124*, 178–187.

Abrahamson, E.E., and Moore, R.Y. (2001). Suprachiasmatic nucleus in the mouse: retinal innervation, intrinsic organization and efferent projections. Brain Research *916*, 172–191.

Aida, R., Moriya, T., Araki, M., Akiyama, M., Wada, K., Wada, E., and Shibata, S. (2002). Gastrin-releasing peptide mediates photic entrainable signals to dorsal subsets of suprachiasmatic nucleus via induction of Period gene in mice. Molecular Pharmacology *61*, 26–34.

Albrecht, U., Sun, Z.S., Eichele, G., and Lee, C.C. (1997). A differential response of two putative mammalian circadian regulators, mper1 and mper2, to light. Cell *91*, 1055–1064.

An, S., Irwin, R.P., Allen, C.N., Tsai, C., and Herzog, E.D. (2011). Vasoactive intestinal polypeptide requires parallel changes in adenylate cyclase and phospholipase C to entrain circadian rhythms to a predictable phase. Journal of Neurophysiology *105*, 2289–2296.

Atkins, N., Mitchell, J.W., Romanova, E. V, Morgan, D.J., Cominski, T.P., Ecker, J.L., Pintar, J.E., Sweedler, J. V, and Gillette, M.U. (2010). Circadian integration of glutamatergic signals by little SAAS in novel suprachiasmatic circuits. PloS One *5*, e12612.

Aton, S.J., Colwell, C.S., Harmar, A.J., Waschek, J., and Herzog, E.D. (2005). Vasoactive intestinal polypeptide mediates circadian rhythmicity and synchrony in mammalian clock neurons. Nature Neuroscience *8*, 476–483.

Brown, T.M., Hughes, A.T., and Piggins, H.D. (2005). Gastrin-releasing peptide promotes suprachiasmatic nuclei cellular rhythmicity in the absence of vasoactive intestinal polypeptide-VPAC2 receptor signaling. The Journal of Neuroscience : the Official Journal of the Society for Neuroscience *25*, 11155–11164.

Chang, Alexander. "Analysis of Circadian Rhythm Using a Novel SCN-Specific Cre Transgenic Mouse Line." The University of Texas Southwestern Medical Center at Dallas. 2010.

Chen, R., Schirmer, A., Lee, Y., Lee, H., Kumar, V., Yoo, S.-H., Takahashi, J.S., and Lee, C. (2009a). Rhythmic PER abundance defines a critical nodal point for negative feedback within the circadian clock mechanism. Molecular Cell *36*, 417–430.

Chen, R., Schirmer, A., Lee, Y., Lee, H., Kumar, V., Yoo, S.-H., Takahashi, J.S., and Lee, C. (2009b). Rhythmic PER abundance defines a critical nodal point for negative feedback within the circadian clock mechanism. Molecular Cell *36*, 417–430.

Cho, H., Zhao, X., Hatori, M., Yu, R.T., Barish, G.D., Lam, M.T., Chong, L., Ditacchio, L., Atkins, A.R., Glass, C.K., et al. (2012). NIH Public Access. *485*, 123–127.

Ciarleglio, C.M., Gamble, K.L., Axley, J.C., Strauss, B.R., Cohen, J.Y., Colwell, C.S., and McMahon, D.G. (2009). Population encoding by circadian clock neurons organizes circadian behavior. The Journal of Neuroscience : the Official Journal of the Society for Neuroscience *29*, 1670–1676.

Colwell, C.S., Michel, S., Itri, J., Rodriguez, W., Tam, J., Lelievre, V., Hu, Z., Liu, X., and Waschek, J. a (2003). Disrupted circadian rhythms in VIP- and PHI-deficient mice. American Journal of Physiology. Regulatory, Integrative and Comparative Physiology *285*, R939–49.

Daly, C., and Ziff, E.B. (1997). Post-transcriptional regulation of synaptic vesicle protein expression and the developmental control of synaptic vesicle formation. The Journal of Neuroscience : the Official Journal of the Society for Neuroscience *17*, 2365–2375.

Eide, E.J., Woolf, M.F., Kang, H., Woolf, P., Hurst, W., Camacho, F., Vielhaber, E.L., Giovanni, A., and Virshup, D.M. (2005). Control of Mammalian Circadian Rhythm by CKI ε -Regulated Proteasome-Mediated PER2 Degradation Control of Mammalian Circadian Rhythm by CKIε-Regulated Proteasome-Mediated PER2 Degradation.

Godinho, S.I.H., Maywood, E.S., Shaw, L., Tucci, V., Barnard, A.R., Busino, L., Pagano, M., Kendall, R., Quwailid, M.M., Romero, M.R., et al. (2007). The after-hours mutant reveals a role for Fbxl3 in determining mammalian circadian period. Science (New York, N.Y.) *316*, 897–900.

Habig WH, Bigalke H, Bergey GK, Neale EA, Hardegree MC, Nelson PG. Tetanus toxin in dissociated spinal cord cultures: long-term characterization of form and action. J Neurochem. 1986 Sep;47(3):930-7.

Hanada, R., Teranishi, H., Pearson, J.T., Kurokawa, M., Hosoda, H., Fukushima, N., Fukue, Y., Serino, R., Fujihara, H., Ueta, Y., et al. (2004). Neuromedin U has a novel anorexigenic effect independent of the leptin signaling pathway. Nature Medicine *10*, 1067–1073.

Hamada, T., Antle, M.C., and Silver, R. (2004). Temporal and spatial expression patterns of canonical clock genes and clock-controlled genes in the suprachiasmatic nucleus. The European Journal of Neuroscience *19*, 1741–1748.

Harmar, A.J., Marston, H.M., Shen, S., Spratt, C., West, K.M., Sheward, W.J., Morrison, C.F., Dorin, J.R., Piggins, H.D., Reubi, J.C., et al. (2002). The VPAC(2) receptor is essential for circadian function in the mouse suprachiasmatic nuclei. Cell *109*, 497–508.

Hastings, M.H., Reddy, A.B., and Maywood, E.S. (2003). A clockwork web: circadian timing in brain and periphery, in health and disease. Nature Reviews. Neuroscience *4*, 649–661.

Hikida, T., Kimura, K., Wada, N., Funabiki, K., and Nakanishi, S. (2010). Distinct roles of synaptic transmission in direct and indirect striatal pathways to reward and aversive behavior. Neuron *66*, 896–907.

Hirano, A., Yumimoto, K., Tsunematsu, R., Matsumoto, M., Oyama, M., Kozuka-Hata, H., Nakagawa, T., Lanjakornsiripan, D., Nakayama, K.I., and Fukada, Y. (2013). FBXL21 Regulates Oscillation of the Circadian Clock through Ubiquitination and Stabilization of Cryptochromes. Cell *152*, 1106–1118.

Hong, H.-K., Chong, J.L., Song, W., Song, E.J., Jyawook, A. a, Schook, A.C., Ko, C.H., and Takahashi, J.S. (2007). Inducible and reversible Clock gene expression in brain using the tTA system for the study of circadian behavior. PLoS Genetics *3*, e33.

Hughes, A.T., Fahey, B., Cutler, D.J., Coogan, A.N., and Piggins, H.D. (2004). Aberrant gating of photic input to the suprachiasmatic circadian pacemaker of mice lacking the VPAC2 receptor. The Journal of Neuroscience : the Official Journal of the Society for Neuroscience *24*, 3522–3526.

Hughes, A.T.L., Guilding, C., Lennox, L., Samuels, R.E., McMahon, D.G., and Piggins, H.D. (2008). Live imaging of altered period1 expression in the suprachiasmatic nuclei of Vipr2-/- mice. Journal of Neurochemistry *106*, 1646–1657.

Kallingal, G.J., and Mintz, E.M. (2007). Gastrin releasing peptide and neuropeptide Y exert opposing actions on circadian phase. Neuroscience Letters *422*, 59–63.

Karatsoreos, I.N., Yan, L., LeSauter, J., and Silver, R. (2004). Phenotype matters: identification of light-responsive cells in the mouse suprachiasmatic nucleus. The Journal of Neuroscience : the Official Journal of the Society for Neuroscience *24*, 68–75.

Kim, J.C., Cook, M.N., Carey, M.R., Shen, C., Regehr, W.G., and Dymecki, S.M. (2009). Linking genetically defined neurons to behavior through a broadly applicable silencing allele. Neuron *63*, 305–315.

Kornhauser, J.M., Nelson, D.E., Mayo, K.E., and Takahashi, J.S. (1990). Photic and circadian regulation of c-fos gene expression in the hamster suprachiasmatic nucleus. Neuron *5*, 127–134.

Kornhauser, J.M., Nelson, D.E., Mayo, K.E., and Takahashi, J.S. (1992). Regulation of jun-B messenger RNA and AP-1 activity by light and a circadian clock. Science (New York, N.Y.) *255*, 1581–1584.

Leak, R.K., and Moore, R.Y. (2001). Topographic organization of suprachiasmatic nucleus projection neurons. The Journal of Comparative Neurology *433*, 312–334.

Leak, R.K., Card, J.P., and Moore, R.Y. (1999). Suprachiasmatic pacemaker organization analyzed by viral transynaptic transport. Brain Research *819*, 23–32.

Lee, J.E., Atkins, N., Hatcher, N.G., Zamdborg, L., Gillette, M.U., Sweedler, J. V, and Kelleher, N.L. (2010). Endogenous peptide discovery of the rat circadian clock: a focused study of the suprachiasmatic nucleus by ultrahigh performance tandem mass spectrometry. Molecular & Cellular Proteomics : MCP *9*, 285–297.

Li, J.-D., Burton, K.J., Zhang, C., Hu, S.-B., and Zhou, Q.-Y. (2009). Vasopressin receptor V1a regulates circadian rhythms of locomotor activity and expression of clock-controlled genes in the suprachiasmatic nuclei. American Journal of Physiology. Regulatory, Integrative and Comparative Physiology *296*, R824–30.

Low-Zeddies, S.S., and Takahashi, J.S. (2001). Chimera analysis of the Clock mutation in mice shows that complex cellular integration determines circadian behavior. Cell *105*, 25–42.

Low-Zeddies, S.S., and Takahashi, J.S. (2005). Mouse chimeras and their application to circadian biology. Methods in Enzymology *393*, 478–492.

Maywood, E.S., Reddy, A.B., Wong, G.K.Y., O'Neill, J.S., O'Brien, J. a, McMahon, D.G., Harmar, A.J., Okamura, H., and Hastings, M.H. (2006a). Synchronization and maintenance of timekeeping in suprachiasmatic circadian clock cells by neuropeptidergic signaling. Current Biology : CB *16*, 599–605.

Maywood, E.S., Reddy, A.B., Wong, G.K.Y., O'Neill, J.S., O'Brien, J. a, McMahon, D.G., Harmar, A.J., Okamura, H., and Hastings, M.H. (2006b). Synchronization and maintenance of timekeeping in suprachiasmatic circadian clock cells by neuropeptidergic signaling. Current Biology : CB *16*, 599–605.

Maywood, E.S., Chesham, J.E., Brien, J.A.O., and Hastings, M.H. (2011). A diversity of paracrine signals sustains molecular circadian cycling in suprachiasmatic nucleus circuits. PNAS.

Mistlberger, R.E., Antle, M.C., Oliverio, M.I., Coffman, T.M., and Morris, M. (2001). Circadian rhythms of activity and drinking in mice lacking angiotensin II 1A receptors. Physiology & Behavior *74*, 457–464.

Moore, R.Y., and Eichler, V.B. (1972). Loss of a circadian adrenal corticosterone rhythm following suprachiasmatic lesions in the rat. Brain Research *42*, 201–206.

Mori, K., Miyazato, M., Ida, T., Murakami, N., Serino, R., Ueta, Y., Kojima, M., and Kangawa, K. (2005). Identification of neuromedin S and its possible role in the mammalian circadian oscillator system. The EMBO Journal *24*, 325–335.

Morin, L.P., Shivers, K.-Y., Blanchard, J.H., and Muscat, L. (2006). Complex organization of mouse and rat suprachiasmatic nucleus. Neuroscience *137*, 1285–1297.

Nakashiba, T., Young, J.Z., McHugh, T.J., Buhl, D.L., and Tonegawa, S. (2008). Transgenic inhibition of synaptic transmission reveals role of CA3 output in hippocampal learning. Science (New York, N.Y.) *319*, 1260–1264.

Nakashiba, T., Buhl, D.L., McHugh, T.J., and Tonegawa, S. (2009). Hippocampal CA3 output is crucial for ripple-associated reactivation and consolidation of memory. Neuron *62*, 781–787.

Nakashiba, T., Cushman, J.D., Pelkey, K. a, Renaudineau, S., Buhl, D.L., McHugh, T.J., Barrera, V.R., Chittajallu, R., Iwamoto, K.S., McBain, C.J., et al. (2012). Young Dentate Granule Cells Mediate Pattern Separation, whereas Old Granule Cells Facilitate Pattern Completion. Cell *149*, 188–201.

Ohsaki, K., Oishi, K., Kozono, Y., Nakayama, K., Nakayama, K.I., and Ishida, N. (2008). The role of {beta}-TrCP1 and {beta}-TrCP2 in circadian rhythm generation by mediating degradation of clock protein PER2. Journal of Biochemistry *144*, 609–618.

Overdick, B., Kirchmair, R., Marksteiner, J., Fischer-Colbrie, R., Troger, J., Winkler, H., and Saria, a (1996). Presence and distribution of a new neuropeptide, secretoneurin, in human retina. Peptides *17*, 1–4.

Pendergast, J.S., Friday, R.C., and Yamazaki, S. (2009). Endogenous rhythms in Period1 mutant suprachiasmatic nuclei in vitro do not represent circadian behavior. The Journal of Neuroscience : the Official Journal of the Society for Neuroscience *29*, 14681–14686.

Preitner, N., Damiola, F., Zakany, J., Duboule, D., Albrecht, U., and Schibler, U. (2002). The Orphan Nuclear Receptor REV-ERB ⎵ Controls Circadian Transcription within the Positive Limb of the Mammalian Circadian Oscillator University of Geneva University of Geneva. *110*, 251–260.

Ralph, M.R., Foster, R.G., Davis, F.C., and Menaker, M. (1990). Transplanted suprachiasmatic nucleus determines circadian period. Science (New York, N.Y.) *247*, 975–978.

Reed, H.E., Meyer-spasche, A., Cutler, D.J., Coen, C.W., and Piggins, H.D. (2001). SHORT COMMUNICATION Vasoactive intestinal polypeptide (VIP) phase-shifts the rat suprachiasmatic nucleus clock in vitro. Neuroscience *13*, 839–843.

Sato, T.K., Panda, S., Miraglia, L.J., Reyes, T.M., Rudic, R.D., McNamara, P., Naik, K. a, FitzGerald, G. a, Kay, S. a, and Hogenesch, J.B. (2004). A functional genomics strategy reveals Rora as a component of the mammalian circadian clock. Neuron *43*, 527–537.

Schoch, S., Deák, F., Königstorfer, a, Mozhayeva, M., Sara, Y., Südhof, T.C., and Kavalali, E.T. (2001). SNARE function analyzed in synaptobrevin/VAMP knockout mice. Science (New York, N.Y.) *294*, 1117–1122.

Schwartz, W.J., Carpino, a, De la Iglesia, H.O., Baler, R., Klein, D.C., Nakabeppu, Y., and Aronin, N. (2000). Differential regulation of fos family genes in the ventrolateral and dorsomedial subdivisions of the rat suprachiasmatic nucleus. Neuroscience *98*, 535–547.

Shearman, L.P., Zylka, M.J., Weaver, D.R., Kolakowski, L.F., and Reppert, S.M. (1997). Two period homologs: circadian expression and photic regulation in the suprachiasmatic nuclei. Neuron *19*, 1261–1269.

Shen, S., Spratt, C., Sheward, W.J., Kallo, I., West, K., Morrison, C.F., Coen, C.W., Marston, H.M., and Harmar, a J. (2000). Overexpression of the human VPAC2 receptor in the suprachiasmatic nucleus alters the circadian phenotype of mice. Proceedings of the National Academy of Sciences of the United States of America *97*, 11575–11580.

Shigeyoshi, Y., Taguchi, K., Yamamoto, S., Takekida, S., Yan, L., Tei, H., Moriya, T., Shibata, S., Loros, J.J., Dunlap, J.C., et al. (1997). Light-induced resetting of a mammalian circadian clock is associated with rapid induction of the mPer1 transcript. Cell *91*, 1043–1053.

Shirogane, T., Jin, J., Ang, X.L., and Harper, J.W. (2005). SCFbeta-TRCP controls clock-dependent transcription via casein kinase 1-dependent degradation of the mammalian period-1 (Per1) protein. The Journal of Biological Chemistry *280*, 26863–26872.

Siepka, S.M., and Takahashi, J.S. (2005). Forward genetic screens to identify circadian rhythm mutants in mice. Methods in Enzymology *393*, 219–229.

Siepka, S.M., Yoo, S.-H., Park, J., Song, W., Kumar, V., Hu, Y., Lee, C., and Takahashi, J.S. (2007). Circadian mutant Overtime reveals F-box protein FBXL3 regulation of cryptochrome and period gene expression. Cell *129*, 1011–1023.

Silver, R., Sookhoo, C.A.A.I., Lesauter, J., Stevens, P., and Lehman, M.N. (1999). Multiple regulatory elements result in regional speci ® city in circadian rhythms of neuropeptide expression in mouse SCN. October *10*, 3165–3174.

Stephan, F.K., and Zucker, I. (1972). Circadian Rhythms. *69*, 1583–1586.

Suh, J., Rivest, A.J., Nakashiba, T., Tominaga, T., and Tonegawa, S. (2011). Entorhinal cortex layer III input to the hippocampus is crucial for temporal association memory. Science (New York, N.Y.) *334*, 1415–1420.

Sujino, M., Masumoto, K., Yamaguchi, S., Horst, G.T.J. Van Der, Okamura, H., Inouye, S.T., and Mc, E. (2003). Suprachiasmatic Nucleus Grafts Restore Circadian Behavioral Rhythms of Genetically Arrhythmic Mice. *13*, 664–668.

Takahashi, J.S., Hong, H.-K., Ko, C.H., and McDearmon, E.L. (2008). The genetics of mammalian circadian order and disorder: implications for physiology and disease. Nature Reviews. Genetics *9*, 764–775.

Tosini, G., Davidson, A.J., Fukuhara, C., Kasamatsu, M., and Castanon-Cervantes, O. (2007). Localization of a circadian clock in mammalian photoreceptors. FASEB Journal : Official Publication of the Federation of American Societies for Experimental Biology *21*, 3866–3871.

Travnickova-Bendova, Z., Cermakian, N., Reppert, S.M., and Sassone-Corsi, P. (2002). Bimodal regulation of mPeriod promoters by CREB-dependent signaling and CLOCK/BMAL1 activity. Proceedings of the National Academy of Sciences of the United States of America *99*, 7728–7733.

Triqueneaux, G., Thenot, S., Kakizawa, T., Antoch, M.P., Safi, R., Takahashi, J.S., Delaunay, F., and Laudet, V. (2004). The orphan receptor Rev-erbalpha gene is a target of the circadian clock pacemaker. Journal of Molecular Endocrinology *33*, 585–608.

Troger, J., Doblinger, A., Leierer, J., Laslop, A., Schmid, E., Teuchner, B., Opatril, M., Philipp, W., Klimaschewski, L., Pfaller, K., et al. (2005). Secretoneurin in the peripheral ocular innervation. Investigative Ophthalmology & Visual Science *46*, 647–654.

Vitaterna MH, King DP, Chang AM, Kornhauser JM, Lowrey PL, McDonald JD, Dove WF, Pinto LH, Turek FW, Takahashi JS. Mutagenesis and mapping of a mouse gene, Clock, essential for circadian behavior. Science. 1994 Apr 29;264(5159):719-25.

Wang, L., Sharma, K., Deng, H.-X., Siddique, T., Grisotti, G., Liu, E., and Roos, R.P. (2008). Restricted expression of mutant SOD1 in spinal motor neurons and interneurons induces motor neuron pathology. Neurobiology of Disease *29*, 400–408.

Welsh, D.K., Takahashi, J.S., and Kay, S. a (2010). Suprachiasmatic nucleus: cell autonomy and network properties. Annual Review of Physiology *72*, 551–577.

West MJ, Slomianka L, Gundersen HJ. Unbiased stereological estimation of the total number of neurons in the subdivisions of the rat hippocampus using the optical fractionator. Anat Rec. 1991 Dec;231(4):482-97.

Yamaguchi, S., Isejima, H., Matsuo, T., Okura, R., Yagita, K., Kobayashi, M., and Okamura, H. (2003). Synchronization of cellular clocks in the suprachiasmatic nucleus. Science (New York, N.Y.) *302*, 1408–1412.

Yamamoto, M., Wada, N., Kitabatake, Y., Watanabe, D., Anzai, M., Yokoyama, M., Teranishi, Y., and Nakanishi, S. (2003). Reversible suppression of glutamatergic neurotransmission of cerebellar granule cells in vivo by genetically manipulated expression of tetanus neurotoxin light chain. The Journal of Neuroscience : the Official Journal of the Society for Neuroscience *23*, 6759–6767.

Yamazaki, S., and Takahashi, J.S. (2005). Real-time luminescence reporting of circadian gene expression in mammals. Methods in Enzymology *393*, 288–301.

Yan, L., and Silver, R. (2002). Differential induction and localization of mPer1 and mPer2 during advancing and delaying phase shifts. European Journal of Neuroscience *16*, 1531–1540.

Yan, L., Takekida, S., Shigeyoshi, Y., and Okamura, H. (1999). Per1 and Per2 gene expression in the rat suprachiasmatic nucleus: circadian profile and the compartment-specific response to light. Neuroscience *94*, 141–150.

Yoo, S.-H., Yamazaki, S., Lowrey, P.L., Shimomura, K., Ko, C.H., Buhr, E.D., Siepka, S.M., Hong, H.-K., Oh, W.J., Yoo, O.J., et al. (2004). PERIOD2::LUCIFERASE real-time reporting of circadian dynamics reveals persistent circadian oscillations in mouse peripheral tissues. Proceedings of the National Academy of Sciences of the United States of America *101*, 5339–5346.

Yoo, S.-H., Mohawk, J.A., Siepka, S.M., Shan, Y., Huh, S.K., Hong, H.-K., Kornblum, I., Kumar, V., Koike, N., Xu, M., et al. (2013). Competing E3 Ubiquitin Ligases Govern Circadian Periodicity by Degradation of CRY in Nucleus and Cytoplasm. Cell *152*, 1091–1105.

Zylka, M.J., Shearman, L.P., Weaver, D.R., and Reppert, S.M. (1998). Three period homologs in mammals: differential light responses in the suprachiasmatic circadian clock and oscillating transcripts outside of brain. Neuron *20*, 1103–1110.